ISTANBUL TECHNICAL UNIVERSITY ★ GRADUATE SCHOOL

EVALUATION OF THERMAL, RHEOLOGICAL, AND DYNAMIC MECHANICAL PROPERTIES OF CNT REINFORCED PEI AND PEEK COMPOSITES: A COMPARATIVE STUDY

M.Sc. THESIS

Fulden KAYGINOK

Department of Materials Science and Engineering

Material Science and Engineering Programme

MARCH 2022

ISTANBUL TECHNICAL UNIVERSITY ★ GRADUATE SCHOOL

EVALUATION OF THERMAL, RHEOLOGICAL, AND DYNAMIC MECHANICAL PROPERTIES OF CNT REINFORCED PEI AND PEEK COMPOSITES: A COMPARATIVE STUDY

M.Sc. THESIS

Fulden KAYGINOK
(521191014)

Department of Materials Science and Engineering

Material Science and Engineering Programme

Thesis Advisor: Assoc. Prof. Hülya CEBECİ

MARCH 2022

İSTANBUL TEKNİK ÜNİVERSİTESİ ★ LİSANSÜSTÜ EĞİTİM ENSTİTÜSÜ

KNT TAKVİYELİ PEİ VE PEEK KOMPOZİTLERİNİN TERMAL, REOLOJİK VE DİNAMİK-MEKANİK ÖZELLİKLERİNİN KARŞILAŞTILMASI

YÜKSEK LİSANS TEZİ

Fulden KAYGINOK
(521191014)

Malzeme Bilimi ve Mühendisliği Ana Bilim Dalı

Malzeme Bilimi ve Mühendisliği Programı

Tez Danışmanı: Assoc. Prof. Hülya CEBECİ

MART 2022

Fulden KAYGINOK, a M.Sc. student of ITU Graduate School student ID 521191014, successfully defended the thesis entitled "EVALUATION OF THERMAL, RHEOLOGICAL, AND DYNAMIC MECHANICAL PROPERTIES OF CNT REINFORCED PEI AND PEEK COMPOSITES: A COMPARATIVE STUDY ", which he/she prepared after fulfilling the requirements specified in the associated legislations, before the jury whose signatures are below.

Thesis Advisor :	**Assoc. Prof. Hülya CEBECİ** Istanbul Technical University	.....
Jury Members :	**Assoc. Prof. Hülya CEBECİ** Istanbul Technical University	.....
	Assoc. Prof. Elif ÖZDEN YENİGÜN Royal College of Art	.....
	Asst.Prof. Alptekin YILDIZ Istanbul Technical University	.....

Date of Submission : 11 February 2022
Date of Defense : 28 March 2022

To my beloved family,

FOREWORD

First of all, I would like to thank my advisor Assoc. Prof. Hülya Cebeci, who inspired me with her work discipline and energy, for trusting me, providing me with many opportunities, guiding me and spending her time and effort.

I sincerely thank Dr. Alptekin Yıldız, who has been tirelessly answering all my questions for three years (I don't think my questions will end in the future :)) and sincerely sharing all his knowledge, from whom I learned a lot and with whom I enjoyed working very much.

I would like to thank Dr. Kaan Yıldız for answering my questions sincerely and courteously, and sharing his knowledge and contributing to my thesis.

I would like to thank dear Dr. İpek Ösken who I enjoy talking for her advice on both academic and daily life (I am still trying to gain a positive perspective :)).

I am especially thankful to my only wingmen, Merve Karabal who helped me throughout my experimental studies and made me happy with her beautiful friendship.

Also, I thank to Suat Ebil for her technical support and kindness, and Dilan Aslan for her help and friendship. I am grateful to all Nanomaterials, Textiles and Advanced Composites Research Group in Aerospace Research Center for their support and friendship, I feel very lucky to be a part of this team.

I would like to thank Deniz Köken and Erdem Kılıçarslan for DSC and SEM analysis.

I would like to thank Özden Güneş Yıldız and Elçin Akar for being my best friends, supporting me and most importantly making me laugh.

Thank you very much to Hakan for motivating me in all areas, for always calling me "go girl" and most importantly for picking me up every time I fall, I'm very lucky and happy to have you in my life, love you.

My last thanks to my beloved family. (Yes, I will write your name one by one :)). My mother Güler, my father Nizam, my sister Pelin, my brother Sercan and my niece Mila, the light of our family, I am very, very lucky to be born into a family with you. Thank you so much for always supporting me and giving me the freedom to decide for my life and making me feel your endless love, I love you so very much!

'Everything we see in the world is the creative work of women.' I commemorate our eternal leader Mustafa Kemal Atatürk, who gave Turkish women the value they deserve, I bow before him with endless respect, gratitude, and love.

March 2022 Fulden KAYGINOK
(Metallurgical and Materials Engineer & Aeronautical Engineer)

TABLE OF CONTENTS

Page

ABBREVIATIONS

1D : 1-Dimensional
2D : 2-Dimensional
ABS : Acrylonitrile Butadiene Styrene
CB : Carbon Black
CF : Crystalline Fraction
CFs : Carbon Fiber
CNF : Carbon Nanofiber
CNT : Multi-walled Carbon Nanotube
DMA : Dynamic-Mechanic Analysis
DSC : Differantial Calorimetry Analysis
EG : Expended Graphite
GNP : Graphene nanoplatelet
GO : Graphene Oxide
HDT : Heat Deflection Temperature
LVR : Linear Viscoelastic Region
MAF : Mobile Amorphous Fraction
PA : Polyamide
PC : Polycarbonate
PEEK : Polyetheretherketone
PEI : Polyetherimide
PMMA : Poly(methyl methacrylate)
PP : Polypropylene
PPS : Polyphenylene Sulfide
PS : Polystyrene
RAF : Rigid Amorphous Fraction
RGO : Reduced Graphene Oxide
SEM : Scanning Electron Microscopy
SWCNT : Single-walled Carbon Nanotube
T_{15} : Degradation Temperature Corresponding to 15% Weight Losses
T_5 : Degradation Temperature Corresponding to 5% Weight Losses
T_g : Glass Transition Temperature
TGA : Thermogravimetric Analysis
T_{hc} : Hot Crystallization Temperature
T_m : Melting Temperature
T_{onset} : Onset Temperature
wt.% : Percentage by Weight

SYMBOLS

$^{\circ}$**C**	**:** Celsius Degree
MPa	**:** Mega Pascal
Pa	**:** Pascal
GPa	**:** Giga Pascal
X_{CF}	**:** Fraction of Crystalline Region
X_{RAF}	**:** Fraction of Rigid Amorphous Region
X_{MAF}	**:** Fraction of Mobile Amorphous Region
ΔH	**:** Heat Fusion Entalpy
ΔC_p	**:** Heat Capacity Change
$\dot{\gamma}$	**:** Shear Rate
G'	**:** Storage Modulus
η^*	**:** Complex Viscosity
η	**:** Shear Viscosity
n	**:** Shear-thinning Exponent
ω	**:** Frequency
T	**:** Temperature
R	**:** Gas Constant
E'_g	**:** Storage Modulus at Glassy Region
E'_r	**:** Storage Modulus at Rubbery Region
$\tan\delta_c$	**:** Tan Delta of The Composite
$\tan\delta_p$	**:** Tan Delta of The Neat Polymer
θ_f	**:** Volume Fraction of The Filler
W	**:** Energy Loss Fraction of The Composite
W_0	**:** Energy Loss Fraction of The Neat Polymer
C_v	**:** Volume of Constrained Region of The Composite
C_0	**:** Volume of Constrained Region of The Neat Polymer

LIST OF TABLES

Page

LIST OF FIGURES

Page

EVALUATION OF THERMAL, RHEOLOGICAL, AND DYNAMIC MECHANICAL PROPERTIES OF CNT REINFORCED PEI AND PEEK COMPOSITES: A COMPARATIVE STUDY

SUMMARY

In this study, the effect of multiwall carbon nanotube (CNT) reinforcement on viscoelastic properties of polyetherimide (PEI) and polyether ether ketone (PEEK) polymers was investigated by oscillator rheology and dynamic mechanical analysis (DMA) method. CNT reinforced PEI and PEEK composites were produced using a specially designed twin-screw extruder at 1, 3, and 5 wt.% at 210 rpm and 360 °C and 380 °C for CNT/PEI and CNT/PEEK composites, respectively. Thermogravimetric (TGA) and differential scanning calorimetry (DSC) analyzes were performed to examine the thermal properties of the samples. It was observed that the decomposition temperatures in PEI samples showed two-stage decomposition depending on the aromatic group and non-aromatic group decomposition at approximately 529 °C and 564 °C, and their thermal stability was found as about up to 400 °C, whereas in PEEK samples, decomposition occurred in a single step due to ether and ketone groups and their thermal stability was found as about up to 550 °C. Also, a residual weight of around 50% in PEI and PEEK samples was at 800 °C. It was seen that CNT did not significantly affect the thermal stability of polymers. In addition, CNT almost did not change the glass transition temperature of polymers (T_g), but it increased the crystal ratio by acting as the nucleation factor for PEEK composites, and the highest crystal ratio was obtained from 1 wt.% CNT/PEEK composite as 29%. The morphological analysis revealed that CNT reinforced PEI and PEEK composites were fabricated homogeneously without any agglomerations. Rheology analysis showed that the linear viscoelastic region (LVR) narrowed with CNT, that is, the critical strain decreased, which was explained as evidence of the formation of a brittle solid network in the structure. Also, the critical strain has an exponential dependence on the volume fraction of the CNT as -1.76 and -1.40 for PEI and PEEK, respectively. On the other hand, the frequency-dependent results in LVR showed that the storage modulus of both polymers increased and the frequency dependence decreased with the increase in the amount of CNT. The frequency dependence of the storage modulus was exponentially 0.7 and 1.57 for neat PEI and PEEK, and these values were calculated as 0.32 and 0.27 at 1 wt.% CNT reinforcement, respectively. The decrease of frequency dependency and sudden increase in 1 wt.% CNT reinforcement was interpreted as an indication of the structure change, and the rheological percolation threshold was determined below 1 wt.% CNT reinforcement was also proved by drawing Cole-Cole plots that are a clear representation for the transition from the liquid-like to the solid-like structure. Additionally, the complex viscosity increased with CNT in both polymers and they changed the behavior from Newtonian to shear-thinning in the low-frequency region

and shear-thinning behavior became dominant with 1 wt.% CNT reinforcement. The lowest shear-thinning exponents were obtained from 5 wt.% CNT/PEI and 5 wt.% CNT/PEEK composites as 0.35 and 0.26, respectively at a frequency range between 10^2 and 10^3 rad/s, by using Power Law. On the other hand, DMA results showed that CNT reinforcement increased the storage modulus of polymers in both glassy and rubbery regions, however, the presence of CNT increased the storage module of PEEK samples more than PEI, this is due to CNT increased the crystal ratio of PEEK and contributes to the elastic portion. Also, the height and the area under the tan delta peak decreased which is the sign of the high interaction between CNT-polymer. Using the DMA results, approaches have also been made to provide a numerical interpretation of the activity of CNT in the polymer and the CNT-polymer interaction and the mobility of the chain by CNT contribution. The decrease in C factor and adhesion factor, and the increase in the degree of entanglement and volume of the constrained region with the presence of CNT were explained as an indication of high interaction and effective reinforcement in CNT/PEI and CNT/PEEK composites. The C factor values were calculated as 0.34 and 0.70, respectively, for 5 wt.% CNT/PEI and 5 wt.% CNT/PEEK composites. Consequently, considering all the results related to viscoelastic properties, it can be said that CNT caused changes in the structure of both PEI and PEEK, and an increase in storage modulus was observed. Moreover, heat deflection temperature (HDT) is extremely critical for the safe operation of polymer structures that will operate at certain temperature changes within specified ranges; thus, HDT of neat PEI and PEEK and their CNT reinforced composites under 0.455 MPa stress were investigated. The highest HDT were obtained from 5 wt.% CNT/PEI and 5 wt.% CNT/PEEK composites at 207 °C and 219 °C, respectively, and it was concluded that CNT improved the thermal properties of PEI and PEEK. This is especially critical for high-performance thermoplastics produced by injection moldings such as PEI and PEEK, as the increase in HDT results in a faster injection process. When the flexural test results of PEI and PEEK samples were evaluated, the flexural modulus of CNT increased by 22% and 28%, in 5 wt.% CNT/PEI and 5 wt.% CNT/PEEK composites as 3.38 and 3.77 GPa respectively. The improvement of the modulus is especially important in terms of improving the performance of polymers used as structural parts and incorporating them into new areas of use. As a result, in this study, CNT reinforced PEI and PEEK composites were successfully produced by the extrusion technique. The effect of CNT on thermal, morphological, viscoelastic, and mechanical properties was discussed in detail with various characterization methods, and when all the results were evaluated, it is seen that CNT improved the viscoelastic properties of PEI and PEEK polymers.

KNT TAKVİYELİ PEİ VE PEEK KOMPOZİTLERİNİN TERMAL, REOLOJİK VE DİNAMİK-MEKANİK ÖZELLİKLERİNİN KARŞILAŞTILMASI

ÖZET

Bu çalışmada, çok duvarlı karbon nanotüpün (KNT) amorf yapılı polieterimit (PEI) ve yarı kristal yapılı polieter eter keton (PEEK) polimerlerinin viskoelastik özelliklerine etkisi osilator reoloji ve dinamik mekanik analiz yöntemi (DMA) ile incelendi. KNT ile güçlendirilmiş PEI ve PEEK kompozitleri, özel tasarlanan çift vidalı ekstrüzyon kullanılarak ağırlıkça %1, 3 ve 5 oranında üretildi. Proses sırasında, KNT ve polimerlerin karıştırılması ekstrüzyon sisteminde farklı bölgelerden eş zamanlı olarak sağlanarak iki besleme adımının da aynı anda bitmesi ile etkin karıştırma hedeflendi. Üretimler, 210 rpm vida dönüş hızında ve KNT/PEI ve KNT/PEEK kompozitleri için sırayla 360 °C ve 380 °C'de gerçekleştirildi. Ekstrüzyondan eriyik olarak karıştırılan numuneler hava soğutması altında çekiciye bağlanarak filaman formunda çekildi ve ardından kırıcı yardımı ile granül haline getirildi. Katkılı ve katkısız granüller kullanılarak ASTM standardına uygun olarak belirlenen geometride DMA için numune hazırlandı. Numuneler, 150x75x3 mm boyutundaki kaset kalıplarda basınçlı kalıplama tekniği ile sıcak preste 300-330 °C sıcaklık aralığında 2,5 MPa basınç altında yaklaşık yarım saat tutularak üretildi. Üretilen numuneler üç eksenli işleme tezgahında 65x13x3 mm boyutlarında kesildi. Bu boyutlarda üretilen numuneler morfolojik özelliklerinin incelenmesi için taramalı elektron mikroskobunda (SEM) ve de termal özellikler için ısı sapma sıcaklığı (HDT) ve mekanik özellikleri için ise eğilme modülü testlerinde kullanılmıştır. KNT ile katkılanmansı sonrasında amorf ve yarı kristalin bir polimerin nano boyutta bir katkıya olan cevabını incelemek ve termal kararlılıklarını belirlemek amacı ile termogravimetrik analiz (TGA) ve diferansiyel tarama kalorimetresi (DSC) analizleri gerçekleştirilmiştir. *TGA*'da, azot atmosferinde 800 °C'ye kadar olan termal davranışları incelenen PEI numunelerinin, iki aşamalı bozunma gösterdiği raporlandı. İlk aşamada, 516 °C'de aromatik grubun bozunması ve sonrasında ise, 540 °C'de aromatik olmayan gruptan kaynaklı bir bozunmanın gerçekleştiği görülmektedir. İncelenen sonuçlarda, katkısız ve KNT katkılı PEI numunelerinin termal kararlılığının yaklaşık 400 °C olduğu saptanmıştır. Azot atmosferinde, 30-800 °C sıcaklık aralığında incelenen PEEK numunelerinde ise, bozunmanın eter ve keton gruplarından kaynaklı olarak tek aşamada gerçekleştiği, katkısız ve KNT katkılı PEEK numunelerinin termal kararlılığının ise 550 °C olduğu belirlenmiştir. Tüm sonuçlar göz önüne alındığında KNT'nin PEI ve PEEK'in termal kararlılığına %1'den %5'e artan ağırlık oranlarında belirgin bir ölçüde etki etmediği görüldü. Diğer taraftan, PEI ve kompozitleri için camsı geçiş sıcaklığının (T_g), PEEK ve kompozitleri içinse hem T_g'nin hem de erime, kristalleşme gibi termal özelliklerinin belirlenmesi amacıyla DSC analizi PEI

numuneleri için 350 °C'ye PEEK'ler içinse 400 °C kadar 2 °C/dk ısıtma hızında yapılmıştır. Yapılan analiz sonucunda, KNT'nin PEI ve PEEK'nin T_g aralığını değiştirmediği görülürken, PEEK kompozitleri için çekirdeklenme faktörü görevini görerek kristalleşme oranını arttırdığı ve en yüksek kristal oranı %29 olarak ağırlıkça %1 katkılı KNT/PEEK kompozitinde elde edilmiştir. Katkısız ve KNT katkılı PEI ve PEEK numunelerinin viskoelastik özellikleri incelemek amacıyla osilator reoloji analizi 360 °C'de gerçekleştirilmiştir. Lineer viskoelastik bölgenin belirlenmesi amacıyla öncelikle 1 Hz frekansta gerinim tarama testi uygulanan numunelerde, KNT miktarının artmasıyla lineer bölgenin daraldığı yani kritik gerinim değerinin düştüğü görülmüştür. Bu durum Payne Etkisi ile ilişkilendirilerek, yapıda kırılgan katı bir oluşumun gerçekleştiğinin kanıtı olarak sunulmuştur. Kritik gerinim değeri ile KNT'nin hacimsel kesri arasında kuvvet yasasının uygulanması ile KNT takviyeli PEI ve PEEK için kuvvet değerleri sırasıyla -1,76 ve -1,40 olarak hesaplanmıştır. Ayrıca, bulunan kritik gerinim değerleri göz önüne alınarak 360 °C'de tüm numunelere 0.1-628 rad/s aralığında frekans tarama testi uygulanmış ve lineer bölgedeki frekansa bağlı viskoelastik özellikler incelendiğinde, KNT miktarının artmasıyla birlikte her iki polimerde de depolama modüllerinde artış görülürken frekansa olan bağımlılık ise azalmıştır. Katkısız PEI ve PEEK polimerlerinde depolama modülünün frekansa olan bağımlılığı ($G' \approx \omega^n$) üstel olarak sırasıyla 0,7 ve 1,57 iken, ağırlıkça %1 KNT katkılamalarında sırasıyla bu değerler 0,32 ve 0,27 olarak hesaplanmıştır. Her iki polimer için de ağırlıkça %1 KNT katkılamasının, modül değerinde ani artışa neden olması ve frekansa bağımlılığı neredeyse ortadan kaldırması sebebiyle yapıda davranış değişimine neden olduğu sonucuna varılmış ve reolojik sızma eşiğinin ağırlıkça %1'in altında olduğu belirlenmiştir. Sıvı benzeri yapıdan katı benzeri yapıya geçişin bu değer aralığında olduğu Cole-Cole eğrileri çizdirilerek de desteklenmiştir. Frekansa bağlı diğer bir özellik olan kompleks viskozite değerleri incelendiğinde ise, KNT'nin polimerin zincir hareketlerini kısıtlaması sebebi ile kompleks viskozitede artışa neden olduğu sonucuna varılmıştır. Katkısız PEI ve PEEK numuneleri, düşük frekans bölgesinde Newton davranışı gösterirken, KNT katkılı numuneler tüm frekans aralıklarında kesme-incelmesi özelliği göstermektedir. Yüksek frekans bölgelerinde kesme incelmesi katsayıları kuvvet yasası ile ilişkilendirildiğinde katkısız PEI ve PEEK'nin n değeri 0,72 ve 0,60 iken ağırlıkça %5 KNT katkılamada bu değerler sırasıyla 0,35 ve 0,26 olarak hesaplanmıştır. Sonuçlar değerlendirildiğinde, artan KNT miktarı ile n katsayısının düştüğü görülmüş ve numunelerin daha belirgin kesme incelmesi gösterdiği sayısal olarak da ispatlanmıştır. Ayrıca katkısız polimerler ile karşılaştırıldığında ağırlıkça %1 katkılamayla, kompleks viskozitedeki ani artış ve düşük frekans bölgesindeki Newton davranışın, kesme incelmesine evrilmesi de reolojik sızma eşiğinin ağırlıkça %1'in altında olduğunun başka bir göstergesi olduğu belirtilmiştir. Diğer taraftan, DMA cihazında çift taraflı mesnet aparatı kullanılarak gerinim tarama testiyle kritik gerinim değerleri bulunan numunelere 1 Hz frekans altında sıcaklık taraması testi uygulanmıştır. Depolama modülü ve tan deltaya göre hesaplanan T_g değerleri incelendiğinde, DSC testi ile aynı doğrultuda sonuçlar elde edilmiş, ve diğer bir ifadeyle KNT'nin PEI ve PEEK'nin T_g'ye olan etkisi bu yöntemle de tespit edilememiştir. DMA sonuçları incelendiğinde, KNT takviyesinin PEI ve PEEK'de camsı bölgedeki ve de kauçuk bölgesindeki depolama modül değerlerini arttırdığı da gözlemlenmiştir. Katkılı ve katkısız PEI ve PEEK numunelerinin T_g'deki depolama modüllerindeki değişimleri karşılaştırıldığın, amorf yapıya sahip PEI numunelerinde PEEK numunelerine göre daha ani bir düşüş görülmüştür. Bu

durumun sebebi, yarı kristal yapıya sahip PEEK numunelerinde henüz kristal erimesi gerçekleşmediğinden yapıda hala hareketsiz davranan bölgelerin olmasıdır, bu sebeple düşüş PEI numunelerine kıyasla daha yumuşaktır. Ayrıca, her iki polimerin de artan KNT miktarıyla tandelta yüksekliğinin düştüğü görülmüştür. DMA sonuçları kullanılarak, KNT'nin polimer içerisindeki etkinliğine ve KNT-polimer etkileşimine ve zincirin KNT katkısı ile mobilite durumuna sayısal bir yorum getirmek için yaklaşımlar da yapılmıştır. C sabiti ve yapışma faktörünün azalışına ve de polimerdeki dolaşıklılık derecesi ve kısıtlanmış bölgenin artışına göre KNT takviyesinin PEI ve PEEK polimerlerinin viskoelastik özelliklerini iyileştirdiği ve KNT-polimer etkileşiminin katkıyla arttığı sonucuna ulaşılır. Buna ek olarak, saf ve KNT katkılı PEI ve PEEK kompozitlerinin depoloma modüllerin incelendiğinde amorf yapılı PEI'de yarı-kristalin PEEK numunelerine göre daha düşük sonuçlar alınmıştır. Bu sonuç, yarı kristal yapıya sahip PEEK numunelerinde rijitliğin kristal bölgeden gelmesi sebebi ile belirlenen T_g civarında kristal erimesi gerçekleşmediğini ve düşüşün az olduğunu göstermektedir. Tüm veriler göz önüne alındığında KNT'nin her iki polimer ile de etkileşiminin yüksek olduğu ve katkılamanın bu polimerlerin viskoelastik özelliklerini iyileştirmesi ile sonuçlanmaktadır. Isı sapma sıcaklığı (HDT), belirli sıcaklık değişimlerinde çalışacak polimer yapıların belirlenen aralıklarında güvenli çalışması açısından son derece kritiktir. Makine parçaları ve performans gerektiren komponentlerde kullanılması planlanan yüksek performanslı plastiklerde HDT'nin tayini, özellikle termoplastik malzemelerin işlenmesi sırasında ısının malzeme üzerindeki etkisinin parça ebatlarına ve toleransına olan etkisi de incelenmelidir. Bu çalışmada PEI ve PEEK polimerlerinin katkısız ve KNT katkılı kompozitleri 0,455 MPa gerilme altında HDT'leri incelenmiştir. En yüksek HDT değerleri ağırlıkça %5 KNT/PEI ve %5 KNT/PEEK kompozitlerinden sırasıyla 207 °C ve 219 °C olarak elde edilmiş ve KNT'nin PEI ve PEEK'nin ısıl özelliklerini iyileştirdiği sonucuna varılmıştır. Bu durum özellikle PEI ve PEEK gibi enjeksiyon kalıplama ile üretimi yapılan yüksek performans termoplastikleri için HDT'nin artışı ile daha hızlı enjeksiyon prosesi ile sonuçlanması açısından kritiktir. PEI ve PEEK numunelerinin eğilme testi sonuçları değerlendirildiğinde ise, KNT'nin modül değerlerinde ağırlıkça %5 KNT/PEI ve %5 KNT/PEEK kompozitlerde sırasıyla %22 ve %28 artarak 3,38 ve 3,77 GPa olarak elde edilmiştir. Modül değerinin iyileşmesi özellikle PEI ve PEEK gibi yapısal parça üretiminde kullanılan polimerlerin performanslarının artması ve yeni kullanım alanlarına dahil edilebilmesi açısından önemlidir. Sonuç olarak bu çalışmada, KNT takviyeli PEI ve PEEK kompozitleri ekstrüzyon tekniği ile başarıyla üretildi. KNT'nin termal, morfolojik, viskoelastik ve mekanik özelliklere etkisi çeşitli karakterizasyon yöntemleriyle ayrıntılı olarak tartışılmakta olup tüm sonuçlar değerlendirildiğinde, KNT'nin PEI ve PEEK polimerlerinin viskoelastik özelliklerini iyileştirildiği görülmüştür.

1. INTRODUCTION

1.1 The Effect of Reinforcement Strategies on The Viscoelastic Properties of The Polymers

1.1.1 Polymer types

The investigation of the viscoelastic properties of polymer composites is not a particularly new area and has been developed for many years, particularly in thermosets. Reinforced thermoset composites have a wide range of applications in aerospace, automotive, biomedical devices, sports, etc., due to high-performance properties [1]. Extensive research has been carried out on epoxy composite systems with different fillers, filler amounts, and modified filler to clarify the potential of reinforcement by analyzing viscoelastic properties. Montazeri et al. examined the effect of 0.1, 0.5, 1, and 1.5 wt.% CNT content on the viscoelastic properties of epoxy using DMA in three-point bending mode at 10 Hz frequency in temperature sweep test [2]. They found that the storage modulus at the glassy region varied with increasing CNT content. In contrast, the highest modulus and increase in T_g were obtained at 0.5 wt.% CNT/epoxy, they stated that increasing CNT amount to 1.5 wt.% CNT/epoxy composite caused agglomeration, thus resulting in a decrease in modulus and T_g. The main reason attributed to these results was due to the interaction between CNT-CNT and CNT-polymer when the CNT concentration was increased by hindering the polymer chain motion as also observed [3]. On the other hand, Fogel et al. explored the effect of CNT concentration from 0 to 1.00% on complex viscosity of epoxy at temperatures of 60, 80, and 100°C [4]. The results showed that only 1 wt.% CNT/epoxy composite had shear thinning behavior at 60°C , while this behavior dominated from 0.50 wt.% to 1.00 wt.% at 80 and 100°C . In addition, they examined the zero shear viscosity and explained that the pattern changed according to being above or below the critical CNT concentration, and stated that the critical value was between 0.25 wt.% and 0.50 wt.%. In the study by Chandrasekaran et

al., the effect of GNP with different weight percentages (i.e., 0.1, 0.3, 0.5, 1, and 2) on the storage modulus and tan delta of epoxy was investigated with DMA [5]. The maximum increase in storage modulus at the glassy region and decrease in tan delta were observed at 0.5 wt.% of GNP/epoxy composite, related to the increase in the crosslink density and the restriction of the movement of the epoxy chains. Moreover, it was declared that a rheological percolation of 0.5 wt.% was achieved in the GNP/epoxy system, indicating the formation of a GNP network. Tang et al. also investigated the effect of weak and strong dispersion of reduced graphene oxide (RGO) on viscoelastic properties and especially on T_g [6]. The results presented that at good dispersion quality, the addition of GNP has increased the storage modulus and T_g due to the dispersed layers leading to a significant interphase region that restricts the mobility of the polymer chains. In another study, the viscoelastic behavior of GNP/epoxy composites with a diameter of 5, and 25 microns (represented as GNP5 and GNP25, respectively) and varying filler amounts was investigated using an oscillating rheometer by Cao [7]. They first performed the strain sweep test, and the results showed that the liquid-like property was dominant in for GNP5 composites in all amount, whereas at 8 wt.% GNP25 composites, the behavior was shifted from liquid-like to solid-like associated with the establishment of a solid GNP network. Then, they applied the frequency scanning test and investigate the structure in detail. Through the increase in GNP, the storage and loss modulus were increased but as in the strain sweep test, the liquid-like feature was dominant in GNP5/epoxy composites, and the solid-like feature was present in the 8 wt.% GNP25/epoxy composite, also it was independent of the frequency. He found that rigid networks started to form at or higher 7 wt.%, resulting in a solid-like elastic behavior. On the other hand, Drzall et al. studied the effect of GNP aspect ratio and concentration on the overall composites [8]. At higher aspect ratios of GNP, when the concentration is increased the storage modulus was enhanced by restricting the segmenatal motion of crosslinks due to interactions between GNP and epoxy. However, compared with lower aspect ratios of GNP, the agglomerated sites hindered the enhancement effect at higher concentrations. Moreover, since the viscoelastic properties and T_g of the polymer is highly dependent on the dispersion quality, surface modification, and size, many studies have been performed to investigate further. Wilkinson and Liu worked on

CNT reinforced epoxy systems through surface modification of CNT. An untreated (pristine-CNT), amino-functionalized (NH-CNT), and base washed (BW-CNT) at different concentrations were studies for their storage modulus at varying frequencies [9]. The results clearly presented that adding CNT for all types increased storage modulus, as specifically as the highest for NH-CNT compared to pristine CNT due to enhanced filler-resin interaction. The percolations of the three different CNT-resin systems were found as NH < BW< pristine CNT proving the effect of dispersion quality on the overall composites by the surface modifications. Since it is widely known that functionalization increases the interaction in the filler-resin system, the viscoelastic properties are also enhanced [10]. In addition, DMA of pristine, NH and BW CNT reinforced epoxy composites at 0.1 wt.% has been studied. They concluded that the functionalization contradicts the effect of viscoelastic properties since the highest storage modulus was obtained from pristine CNT. However, Kim et al. explained that functionalization increased the interaction between CNT and resin due to preventing the mobility of chains, claiming that the stability of the modulus value as a function of temperature has been increased [11]. In the literature, there are many studies on carbon-based materials other than CNT and graphene derivatives, and even the viscoelastic properties of epoxy composites produced with various ceramic and organic fillers have also been studied in details [12–15]. Moreover, not only the viscoelastic properties of epoxy-based composites but also vinyl ester and polyester-based composites have been extensively studied in the literature [16]. Davis and co-workers worked on the rheological behavior of CNT in unsaturated polyester resin (UPR) by using an oscillatory shear rheometer [17]. They stated that the addition of CNT increased both the storage modulus and loss modulus values, and the percolation threshold was in the range of 0.10 and 0.16 vol.% CNT.

As of literature findings, it was obvious that the viscoelastic properties of thermosets when a nanofiller is present have been widely studied. However, for the next generation composites and advanced structures, it is of interest to define the characteristics of high-performance thermoplastics when reinforced with nanofillers. Ease of production, multifunctionality, recyclability and sustainability are the major driven forces to create such advanced materials for autiomative, aerospace, and marine industries [18,19]. However, still a lack of fundamental scientific knowledge is missing

when different polymers are being used as the matrix materials. The polymer as related to the chain type is also critical to understand when these nanoscale fillers are being employed. The effect of nanoscale filler on the overall reinforcement potential should be addressed in details with a tool such as dynamic mechanical analysis. Amorphous thermoplastic polymers, randomly arranged, do not have a crystalline region. These polymers only exhibit a T_g and soften above the T_g [20]. Polymers such as acrylonitrile butadiene styrene (ABS), poly(methyl methacrylate) (PMMA), polystyrene (PS), and PEI are some examples of them. Adding reinforcements such as CNT to an amorph polymer is expected to create differences on the mechanical properties of the composites, however the effective mechanisms should also be addressed when chain configurations are considered. Singh et al., studied the dynamic mechanical properties of CNT reinforced ABS composites in detail by using various analytical tools to provide a representation of filler-polymer interaction [21].They found that the storage and loss modulus of CNT/ABS composites were increased whereas the damping factor decreased. Morever, T_g has shifted to higher temperatures with the addition of CNT. They concluded the degree of entanglement and b factor values increased up to 5 wt.% CNT addition referring as an optimum value for enhancement capability from the filler. On the other hand, Yang et al., characterized oscillatory rheology properties of GNP/ABS composites with various GNP volume fractions [22]. First, they determined linear viscoelastic region (LVR) by applying strain sweep test and presented the Payne effect at a sudden reduction through the increased strain when the GNP network is destroyed. Also, the frequency dependency on the both storage and loss modulus is less pronounced when the GNP content is increased supporting a solid-like formation aligned with a decrease in tan delta. Winey et al., worked on single walled carbon nanotube (SWCNT) reinforced PMMA composites for dynamical mechanical properties [23]. They found that storage and loss modulus increased with increasing SWCNT and storage modulus was almost independent after 0.2 wt.% SWCNT addition resulting a transition from liquid-like to solid-like behaviors that hinders the polymer chain motion. Also, rheological percolation threshold was calculated as 0.12 wt.% by using power-law relation. Pataki et al. investigated the rheological behavior of CNT (called MWCNT in here)/PS and reached solid-like behavior inclined to dominate between 1 and 2 wt.% CNT loading, referring as a

sign of rheological percolation threshold (Fig. 1.1) [24]. Also, they found that with the CNT addition, CNT/PS composites showed shear-thinning behavior clearly. The results were supported with a pattern in Cole-Cole diagram and a decrease in tan delta. On the other hand, Bruck et al. observed solid-like behavior after 2 vol.% CNT content in PS, and McClory et al. reported the percolation threshold between 3 and 5 wt.% CNT [25, 26].

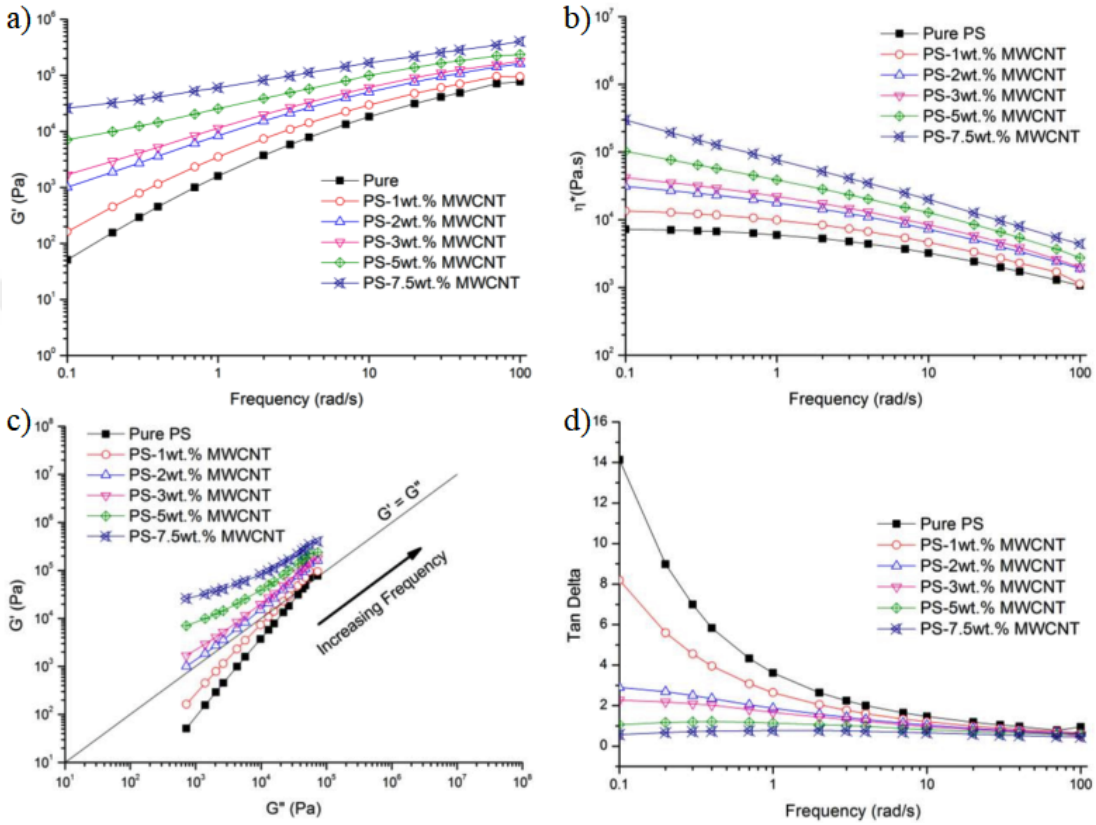

Figure 1.1 : Rheological results of MWCNT/PS composites [24].

Pötschke et al. [27]. studied the CNT reinforced polycarbonate (PC) polymer nanocomposites by rheological analysis. The CNT addition to PC has resulted an increased complex viscosity after 2 wt.% CNT addition, where no Newtonian plateau at low frequency was observed (Fig. 1.2). The sudden increase in storage modulus was associated with the significant increase in viscosity. Also, they observed that after 1 wt.% CNT, the slope of the storage modulus changed significantly and became frequency-independent after 5 wt.% CNT content attributing to an enhanced interaction between CNT-CNT through forming an interconnected structure. The results have been supported through pattern changes on the modified Cole-Cole

diagram. Oppose to those results, Kim et al. analyzed the viscoelastic properties of CNT reinforced PC in DMA and reported that the glassy region did not present a significant change when CNT concentration [28]. However, the viscoelastic properties were increased in rubbery region accompanied with a tan delta decrease due to the confined PC chain.

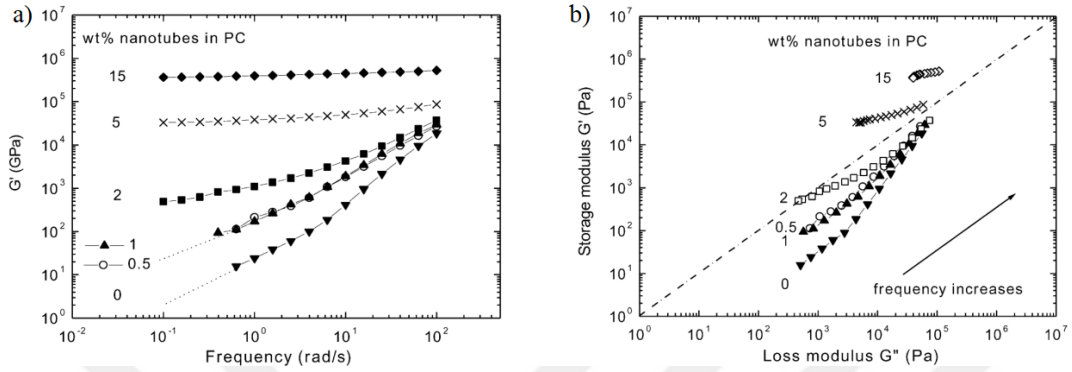

Figure 1.2 : Rheological results of CNT/PC composites [27].

Furhtermore, Isayev et al. investigated the effect of molecular weight on rheological behaviour for CNT reinforced PC composites. The low molecular weight PC (represented as CNT/LPC) and high molecular weight PC (represented as CNT/HPC), were studied at various CNT loadings respectively [29]. They reported LPC and HPC composites showed similar patterns in storage modulus and tan delta, also found value of percolation threshold as 0.102 vol. and 0.0619 vol.% , respectively. The lower percolation for LPC was referred to smaller filler-filler distance to restrict the chain motion of the polymer.

Moreover, Isayev et al. examined the rheological behavior of pure PEI and CNT/PEI (from 1% to 10% by weight) [30]. The dynamic mechanical analysis were performed at oscillatory shear mode and presented that up to 2 wt.% CNT loading, a Newtonian plateau in all composites as in neat PEI were observed, however, beyond 2 wt.% CNT a strong shear thinning behavior dominated the polymer nanocomposite at low-frequency region. They claimed that a sharp increase in complex viscosity between 1 and 2 wt.% may be possible as representing the rheological percolation. Additionally, storage modulus exhibited plateau region after 2 wt.% which indicating solid-like behaviors meaning polymer chain motion is restricted by CNT in long-chain dynamics. On the other hand, CNT affected polymer chain relaxation, which supported a decrease in tan delta value with increasing CNT loading. In connection with this

study, linear rheological behaviors of CNT/PEI composites at different CNT weight fractions was further evaluated by Cebeci et al. [31]. As shown in the (Fig. 1.3), neat PEI and all CNT/PEI composites showed frequency dependent-shear thinning, however 5 wt.% CNT/PEI composite showed both stronger shear thinning and higher increment in complex viscosity. In addition, neat PEI and CNT/PEI composites exhibited viscous behavior at low weight fractions, whereas 5 wt.% CNT/PEI behavior was elastic. This phenomenon was associated with rheological percolation and the threshold value was found between 0.25 and 5 wt.%.

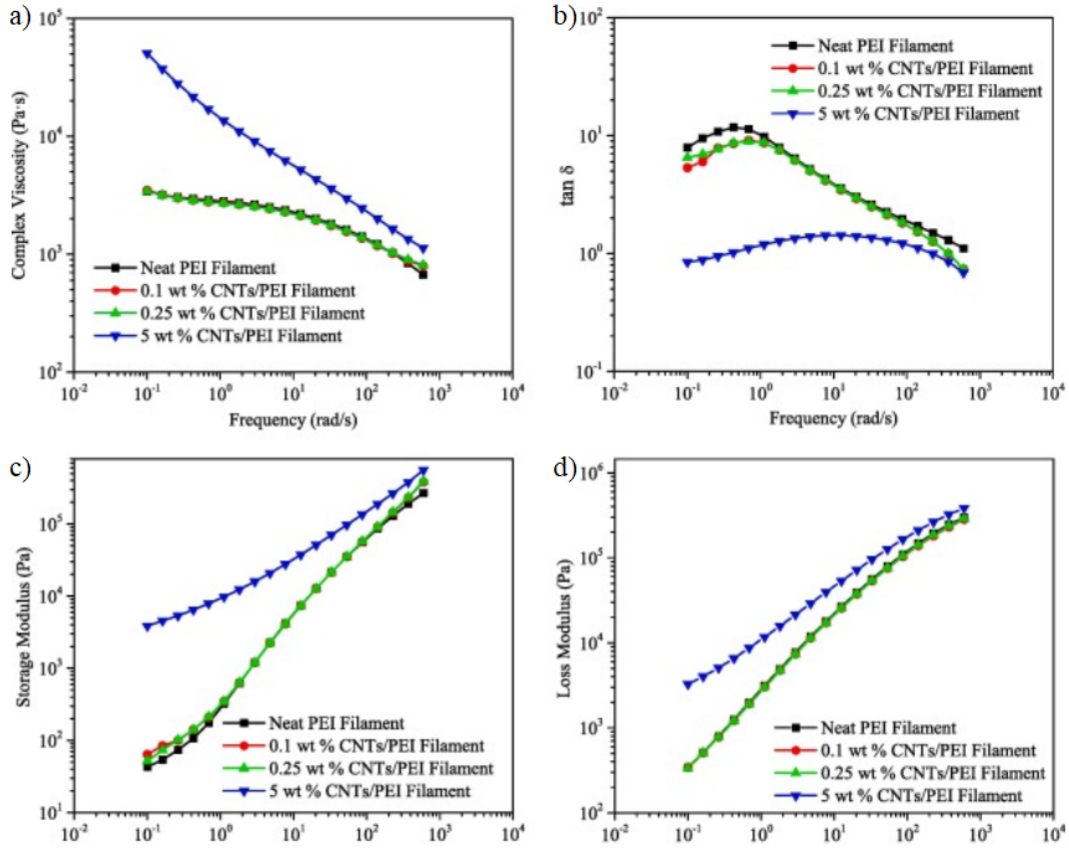

Figure 1.3 : Rheological results of CNT/PEI composites [31].

The investigation regarding dynamic mechanical properties of 0.5 and 1 wt.% CNT/PEI nanocomposite film was performed by Liu et al [32]. They reported storage modulus increased with CNT loading and even 1 wt.% CNT/PEI nanocomposite film improved storage modulus and T_g by 9°C and 146%, respectively, attributed these improvements to the CNT's restriction of chain movements.

While the viscoelastic behavior of amorphous polymers is explained extensively in earlier sections, the addition of nanofillers to semi-crystalline polymers is also further

studied in literature [20]. Choudhary et al. studied on linear viscoelastic behavior of CNT/polypropylene (PP) composites having 0.2-7.0 vol. % filler content [33]. The composites showed terminal behavior until the addition of 0.4 vol.% CNT, after which this behavior disappeared and the frequency dependence weakened, which was explained as evidence that polymer relaxation was restrained by CNT. They reported that composites showed solid-like behavior in between 1.8 and 7 vol.% in the all frequency ranges and found the rheological percolation threshold as 0.27 vol.%. They then examined the dynamic mechanical properties of the CNT/PP composites and calculated the filler effectiveness parameter, C factor and degree of entanglement. They explained that the decrease in the C factor and the increase in degree of entanglement with the increasing amount of CNT indicate the interaction between CNT and PP. In another study, Shim et al. studied the rheological properties of SWCNT/PP at a filler amount of 0.29 to 6.56 wt.% [34]. The addition of SWCNT increased the complex viscosity and storage modulus by making them frequency independent, referring to an interconnected SWCNT network in the PP. 0.29 wt.% SWCNT loading was found to be a rheological percolation threshold supported by a change in phase angle.

Goodridge et al. worked on rheological properties of 0.1 and 0.2 wt.% CNT addition in polyamide (PA) composites [35]. Neat PA and its composites showed liquid-like behavior in all frequencies and CNT addition in small fraction increased storage modulus slightly, but changed the dependency of frequency neat PA which indicated CNT-polymer and CNT-CNT interactions. In addition, it was observed that the viscosity values increased with the addition of CNT and the shear thinning feature became more pronounced. This was explained by dispersion quality of CNT and the inhibition of chain movements of PA when CNT present. Morever, Liu et al. [36] studied the CNT/PA composites and found that addition of CNT, also increased the the complex viscosity, where the shear thinning became more dominant, hence storage modulus were independent from the increased frequency. In addition, it was concluded that CNT reinforcement affects the long-range dynamic properties of the polymer, but not the short-range. Additionally, Daver et al., explored the rheological properties of GNP/PA composites and achieved the highest increase instorage modulus at 17 wt.% GNP/PA [37]. The rheological percolation was also reported to be between 6 and 10 wt.% GNP loading, and was supported by the Cole-Cole diagram.

Kim et al. evaluated viscoelastic properties of CNT/polyphenylene sulfide (PPS) composites with different CNT weight fractions [38]. A sudden increase in both the complex viscosity and storage modulus was observed with the addition of 3 wt.% CNT and the rheological percolation value was reported to be close to 3 wt.%. When SWCNT was considered in both semi-crystalline PPS and PEEK polymers, Diez et al explored the concentration effect [39]. The storage modulus and complex viscosity were all increased for PPS and PEEK composites an increase in SWCNT. However, the decrease in frequency dependence of PEEK storage modulus was more evident. In addition, the rheological percolation of PEEK composites was found to be significantly lower than that of PPS composites, indicating that SWCNT interacts better with PEEK. Diez-Pascual and coworkers studied the dynamic mechanical behavior of SWCNT/PEEK composites [40]. It is reported that 1 wt.% SWCNT increased by 37% in storage modulus and loss modulus shifted higher temperatures, which suggested that SWCNT hinders the local motions of the ketone groups. Fernández-Blázquez evaluated frequency dependent viscoelastic properties of GNP/PEEK composites at 1, 5 and 10 wt.% GNP loading [41]. Complex viscosity of neat PEEK and 1 wt.% GNP presented a Newtonian behavior, while 5 and 10 wt.% GNP/PEEK composites exhibited shear thinning and viscosity values increased significantly. In addition, the storage values increased with GNP loading and it was clearly seen that a rubbery region was formed in 5 and 10 wt.% GNP composites, which indicates that the GNP network was formed. In another similar work, dynamic mechanical analysis of GNP/PEEK fiber composites was performed in tension mode and it was reported that the storage modulus value increased with the addition of GNP [42]. Bangarusampath and coworkers prepared CNT (called MWCNT in here)/PEEK composites up to 17 wt.% filler content [43]. Strain sweep test results showed that storage modulus increased and critical strain values decreased with CNT loading, attributed with Payne effect. Then, they analyzed frequency-dependent properties and observed CNT addition increased both complex viscosity and storage modulus (Fig. 1.4). Beyond 1 wt.%, terminal behavior in composites disappeared and they exhibited plateau like regime which related with translation from liquid like to solid like behaviors and thus, the critical threshold concentration was determined as around 1 wt.% CNT.

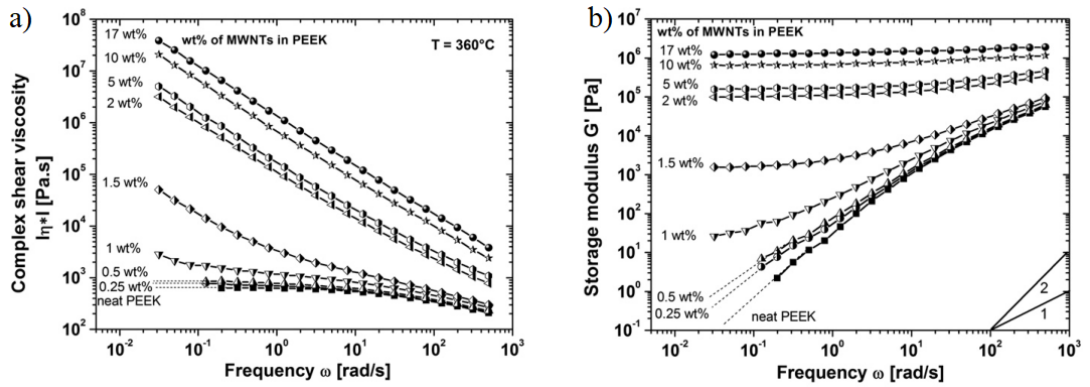

Figure 1.4 : Rheological results of CNT/PEEK composites [43].

As a result, the effect of carbon-based reinforcements such as CNT and GNP on the viscoelastic properties of several polymers has been extensively studied. The majority of these studies focused on thermoset based polymer composites, since many industrial applications are of this kind. However, a transition from thermosets to thermoplastics is being considered for many advanced applications in several industrial such as aerospace, biomedical and marine. Hence, it is still required to investigate the viscoelastic properties of high performance polymers such as PEI and PEEK for advanced applications when the reinforcements are used.

1.1.2 Filler types

Carbon-based materials such as carbon black (CB), carbon fiber (CFs), carbon nanofiber (CNF), singlewall carbon nanotubes (SWCNT), multiwall carbon nanotubes (CNT), graphene nanoplatelets (GNP) exhibit promising features in polymer composites due to their unique functional features such as higher aspect ratio, surface area, mechanical, thermal, and electrical properties, etc. than conventional materials (Fig. 1.5) [44].

The first of these materials, CB, is composed of small spherical carbon particles having 100 nm in diameter which creates network structure by joining together [45]. There are many studies in the literature, especially on CB added elastomers, also the effect of viscoelastic properties of CB used as reinforcement material in various thermoplastics such as ABS, PP, PC and thermoset such as epoxy has been investigated [46]. It has been reported CB creates a reinforcement effect and causes both change in structure and increase in viscosity due to the hydrodynamic effect in polymers [46–49].

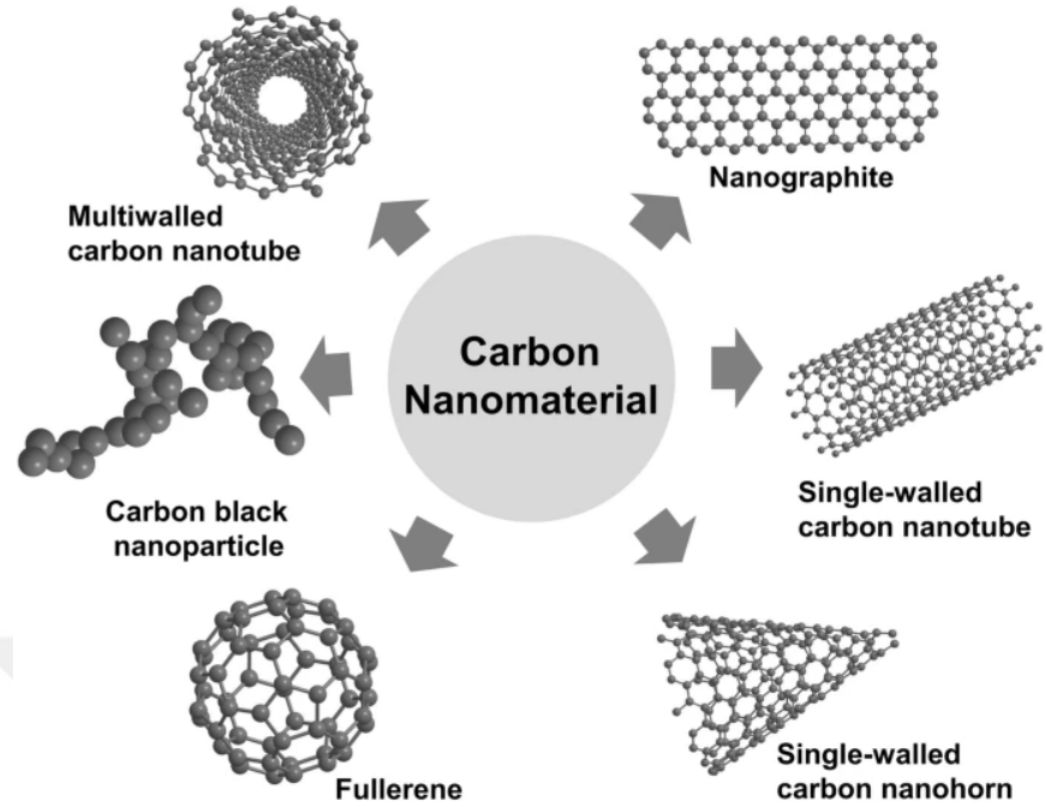

Figure 1.5 : Carbon-based materials [44].

Another well-known carbon-based material is CFs, which is one of the widely used reinforcing materials in composite production, especially in aerospace application with epoxy. CFs with micro size has a low aspect ratio and more defects among other carbon-derived materials due to its high diameter [50]. There are rheological studies especially on chopped CFs polymer composites [51].

CNF is one of the most common members of CFs with a 1-dimensional cylindrical shape, with an average diameter of 70-200 nm and 50-200 micrometers, respectively. Compared with CNT, it has lower surface area and higher defects [52–54]. Studies on the viscoelastic properties of CNF reinforced polymer composites are more limited compared to other carbon-based materials [55].

Another carbon-based material is 2-dimensional (2D) graphene, which consists of a single carbon layer with a hexagonal structure. Graphene, which is preferred as a reinforcing material in many different polymers due to its high aspect ratio and surface area, has many different derivatives such as GNP, graphene oxide (GO), RGO. The viscoelastic properties of graphene-based composites have been studied in detail in the literature [5, 42, 56]. Despite having a high aspect ratio, GNP with agglomeration

problem may not have the expected effect on rheological properties when it cannot be dispersed effectively [8].

Another remarkable carbon-based material is 1-dimensional (1D), tube-shaped, nano-sized carbon nanotubes. Carbon nanotubes can consist of a single graphene layer are called SWCNT, or more than one-layer number called CNT having higher purity. They are often preferred as reinforcement materials due to their excellent thermal, electrical and mechanical properties [57].

As mentioned above, there are many detailed studies on the effect of carbon-based materials on the viscoelastic properties of various polymeric materials, but in articles in which different carbon-based materials are reinforced and compared to the same polymer, the effect of dimension difference, that is, the effect of aspect ratio and surface area, on viscoelastic properties is understood more clearly.

Durmuş and coworkers evaluated the rheological properties of CB and CFs cyclic olefin copolymer (COC) composites [58]. It was found that the rheological percolation value of CB/COC composites was lower than that of CFs/COC composites, and at the same time the yield values at complex viscosity were higher, and this result was associated with the higher surface area and nano-size of CB. In another study conducted by this team, dynamic mechanical analyzes of CB and CFs/COC composites were performed and it was reported that since the aspect ratio of CFs is higher, its effectiveness in the composite was also higher [59].

Isayev et al. produced CNT, GNP, and CB/PP composites at different filler loading and clarified the effect of filler types on rheological properties of composites [60]. Results showed that storage modulus and complex viscosity values increased with filler addition for all composites. The highest increment in storage modulus and viscosity values was obtained from CNT/PP composites, followed by CB/PP and GNP/PP composites at the same filler loading. It was associated with higher surface area and aspect ratio of CNT, i.e. as aspect ratio and surface area increase, more substantial dispersion and polymer-filler interaction were achieved.

Mark and coworkers conducted another study supporting these results. They worked on rheological comparison of CB, expanded graphite (EG), and CNT (called MWCNT in here) /PC composites [61]. The highest increment in complex viscosity was obtained from CNT/PP composites, CB and EG. When the behavior in viscosity was examined,

CB/PC, CNT/PC, and EG/PC composites showed a change in 4 wt.%, 2 wt.%, and 10 wt.% addition, respectively (Fig. 1.6). It was the evidence of rheological percolation and explained as the lowest percolation threshold values were obtained from CNT/PC composites. Examining composites 4 wt.% filler loading were analyzed, while the complex viscosity value of CNT/PC composites was high at low frequency, that of CB/PC and EG/PC composites at high frequency was high, this is due to the strong shear thinning properties of CNT/PC composites. As a result of this study, it was concluded that the best improvements were obtained in CNT/PC composites.

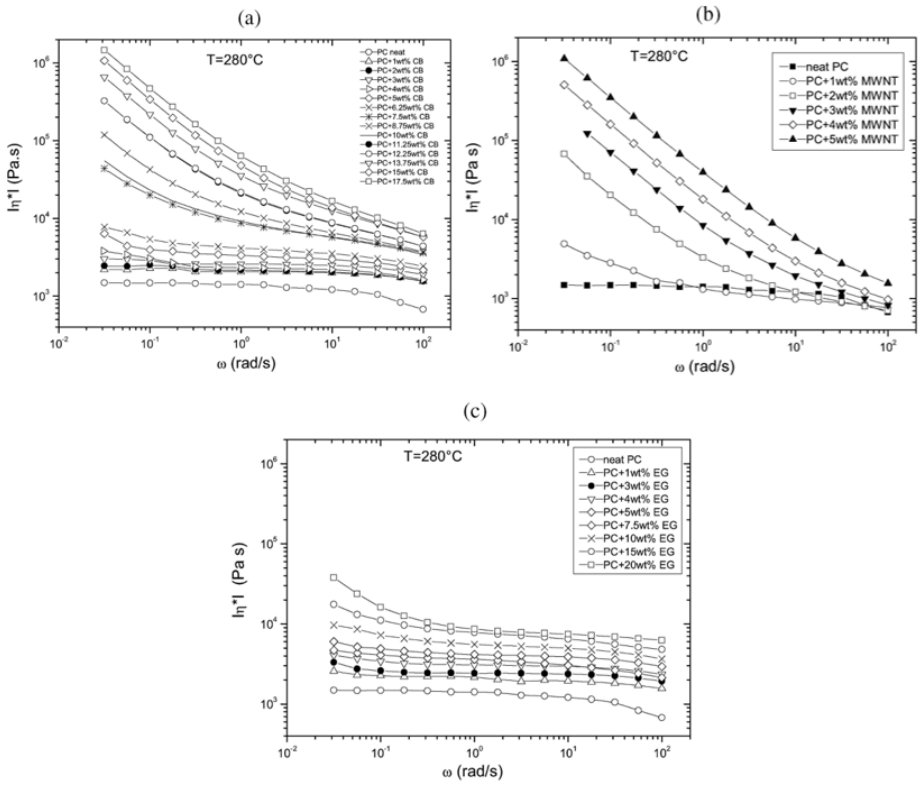

Figure 1.6 : Rheological results of CB/PC, CNT/PC, and EG/PC composites [61].

In line with the above results, Lin et al. investigated the rheological properties of CNT, CB and GNP reinforced PP composites at the same filler ratio in dynamic shear rheology and stated that the increase in complex viscosity was highest in CNT reinforced due to high aspect ratio [62]. Another supportive study was carried out by Sumfleth et al. [63]. They found that rheological percolation threshold of CNT/epoxy and CB/epoxy composites were 0.2 and 0.8 wt.%, respectively, and they explained that these results were due to the aspect ratio differences. On the contrary, Deng et al. observed a no clear difference for the viscosity of CNT and CB reinforced PP composites when similar filler concentrations were used. This

results was inline with Pötsche et al. studies where the rheological properties depend not only on the interaction between fillers but also on the filler-polymer and polymer-polymer interactions [64, 65]. Palacios et al., evaluated the rheological behavior of CNT/GNP/PA, both binary and hybrid composites [66]. Results showed that CNT/PA composites showed non-terminal behavior, while GNP/PP composites showed terminal behavior at 4 wt.% filler loading due to the dimensional differences of CNT and GNP. It was explained that CNT having 1D structure have a high ability to establish interconnected solid networks, but GNP have difficulty establishing particle-particle interaction due to their sheet-like structure and promoting the slipping and thus can not prevent polymer motion. Also, they investigated two different types of GNP in terms of size, surface area, and thickness on PP rheology. GNP having high surface area and small size has a higher impact on rheological properties. Similar to previous work, Disdier and coworkers investigated the effect of GNP having different viscoelastic properties of PP [67]. They reached that a higher increment in storage modulus depending on temperature and complex viscosity was obtained from GNP/PP samples having the lowest diameter and thickness. In addition, this aspect of the research was compiled by Cassagnau et al. in the study that increasing the aspect ratio reduces the maximum packing fraction and causes an increase in viscosity (Fig. 1.7) [68].

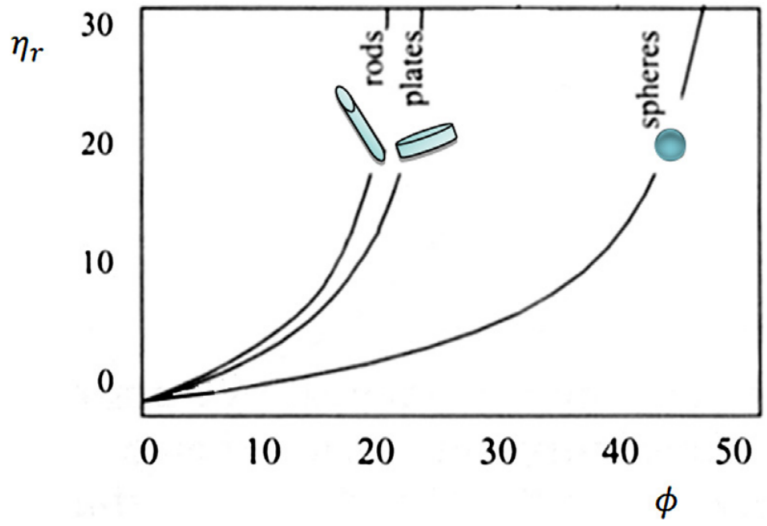

Figure 1.7 : Comparison of packing fraction versus viscosity graph of different fillers [68].

In addition to the results obtained by experimental studies, there are also simulation studies on the reinforcement effect in the literature. Knauert et al. made theoretical

simulations on dimensional differences of the filler material on viscosity [69]. In the system, the nanoparticles were modeled as well dispersed in the polymer, but the sheet-like structure was not well dispersed, as can be seen in Fig. 1.8. They explained that 1D rod-like shaped as CNT assisted higher increment in viscosity than 2D sheet-like shaped as GNP; they associated this result with the more remarkable ability of 1D structures to interact with each other (Fig. 1.9). Also, in this modeling, the contact ratio of particles between particle and polymer chains was calculated for different geometries. They obtained the highest fraction for both fractions from rod-like particles.

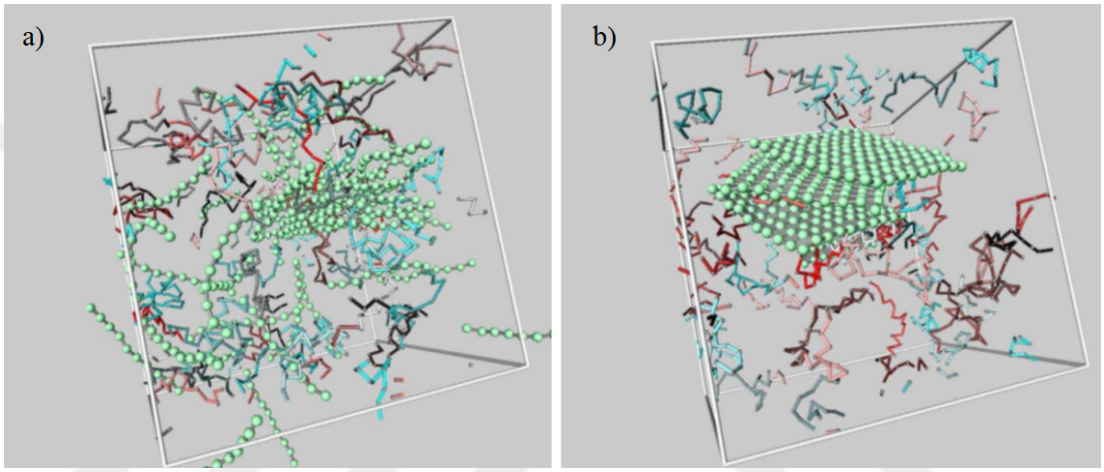

Figure 1.8 : Dispersion simulations of (a) rod-like, (b) sheet-like structure [69].

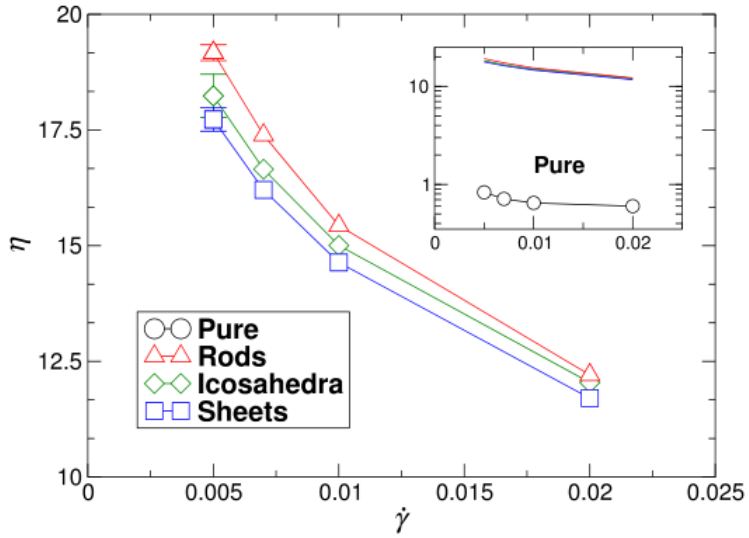

Figure 1.9 : Viscosity versus shear rate graph of composites having different geometries [69].

Consequently, various carbon-based reinforcements have been used to improve viscoelastic properties. It has been observed that the interactions of reinforcement materials with different shapes, sizes and surface areas with polymers are also different. Considering all the studies, 1D CNT is seen as a more promising material than other reinforcement materials. It improves even at low additive amounts thanks to its high surface area and aspect ratio.

1.2 Motivation

Polymeric materials in particular thermoplastics are viscoelastic materials. When advanced applications are considered, high-performance thermoplastics are important candidates for several applications such as load-bearing components, vibrational dampers, and shock absorbers. To design and analyze thermoplastic composites, it is essential to understand the viscoelastic properties of them. The thermo-mechanical behavior of high-performance thermoplastics such as PEI and PEEK has attracted substantial attention especially when fillers in nano and micro scale are considered. Understanding the interaction between the filler-polymer, polymer-polymer and filler-filler will help to develop novel material systems for specific applications. The aim of this study is to explore the viscoelastic properties of PEI and PEEK when a carbon-based nanomaterial such as carbon nanotubes (CNT) is present. Since CNT is a high aspect ratio filler, the effect of polymer type being for PEI as amorphous and PEEK as semi-crystalline is further studied to reveal the effect of chain type. PEI and PEEK composites were produced with different CNT concentrations to analyze the effect of the presence of the CNT on the thermal, morphological, viscoelastic, and mechanical properties of PEI and PEEK. The strain-dependent and frequency-dependent viscoelastic properties of the composites were investigated in detail by employing with Payne effect, percolation theory, and Cole-Cole analysis. Also, change in thermo-mechanical properties with the presence of the CNT were examined in DMA by conducting calculation of C factor, degree of entanglement, adhesion factor, and volume of the constrained region, which enable to examine CNT-polymer interaction effectively. In conclusion, we tried to fill the gap in the

literature by investigating the viscoelastic properties of CNT reinforced PEI and PEEK composites at both the oscillator rheology and DMA.

1.3 Overview of the Thesis

In this thesis, which consists of four main parts, we worked on revealing the viscoelastic properties of CNT reinforced PEI and PEEK using oscillating rheological analysis and DMA. Background information about viscoelastic properties of polymer composites in two subsections as polymer types and filler types, were reviewed in Chapter 1. The specifications of the materials, processing techniques & conditions, and characterization methods were presented in Chapter 2. The change in morphological, thermal, viscoelastic and mechanical properties of the PEI as amorphous and PEEK as semi crystalline with presence of CNT were discussed and the CNT-PEI and CNT-PEEK interactions were further explored with oscillatory rheology analysis and DMA by using some approaches in Chapter 3 and finally, the entire thesis work was summarized in Chapter 4.

2. EXPERIMENTAL

The effect of CNT reinforcement on an amorphous and a semi-crystalline polymer plays a crucial role on the overall mechanical and thermal properties. In this thesis, neat and CNT reinforced PEI and PEEK polymers were fabricated to investigate the CNT reinforcing effect on different chain configurations. In Fig. 2.1 the road map of the thesis is demonstrated. An extensive characterization of the polymer nanocomposites was performed to reveal the effect of CNT when an amorphous and a semi-crystalline polymeric chains were considered.

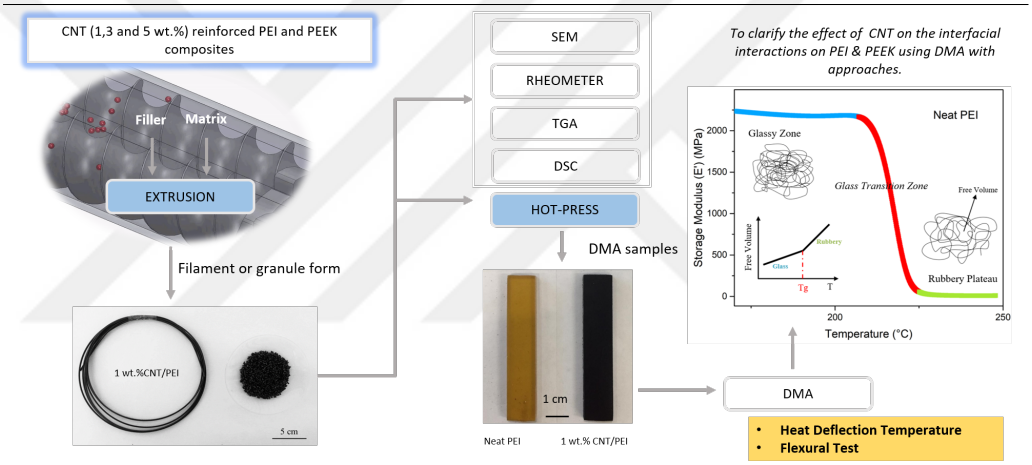

Figure 2.1 : Road map of the thesis.

2.1 Materials

An industrial scale multi-walled CNT were used as reinforcing filler for polymer nanocomposite fabrications. The CNT were supplied from Nanokomp with 10-20 nm in diameter, 1.5-2 μm in length, and having 90% purity. An amorphous PEI and semi-crystalline PEEK, referred as high performance polymers were used as matrix materials (Fig. 2.2). PEI granules were purchased from Sabic (Ultem 1010) with glass transition temperature of 217°C, and density of 1.27 g/cm^3. PEEK granules were purchased from Vitrex (450G) with glass transition temperature of 143°C, melting temperature of 343°C and density of 1.30 g/cm^3. Molecular structure of the polymers were given in Fig. 2.3. All materials were used without treatment during processing.

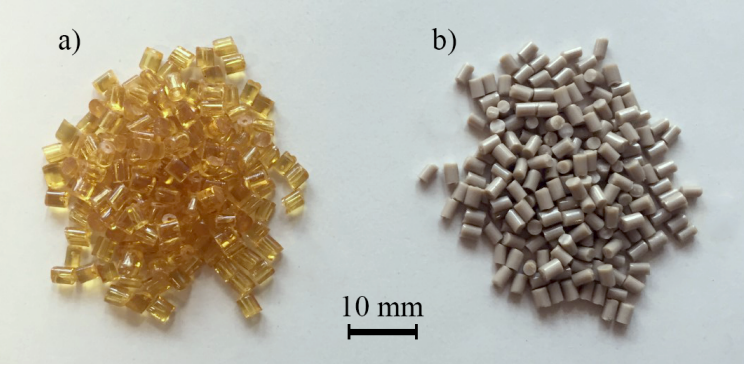

Figure 2.2 : Granules of (a) PEI and (b) PEEK.

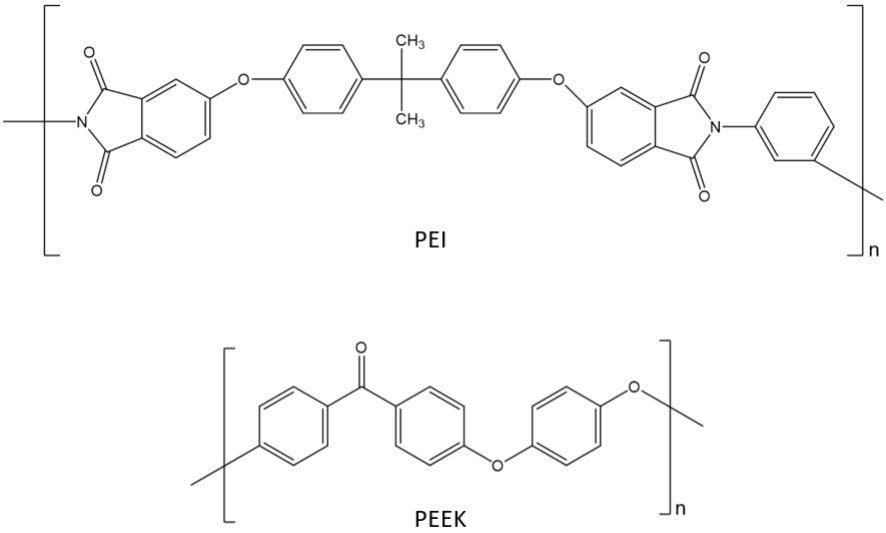

Figure 2.3 : Chemical structure of (a) PEI and (b) PEEK.

2.2 Fabrication

CNT reinforced PEI and PEEK composites were fabricated with 1, 3, and 5 wt.% by using a custom-made co-rotating twin-screw extruder with 22 in length to diameter screw ratio (L/D) designed by Kökbir Import&Export. The technical information of the extruder was given in Table 2.1. Before the fabrication, all polymers were dried in an oven at 150°C overnight to remove water accumulation. During the processing, CNT and all polymers were fed to the same zone from separate hoppers in a cycle (see Fig. 2.4). Process parameters of CNT/PEI and CNT/PEEK composites were tabulated in Table 2.2. The whole experiment was shown in Fig. 2.5. To perform a comparison in between the polymers, all processing conditions were kept constant except the process temperatures as related with their T_g.

Table 2.1 : Specification of twin-screw extruder.

Properties	Twin-screw extruder
Number of screws	2
Screw diameters	12 mm
Screw material	Nitrified carbon steel
L/D ratio	22
Rotation	Co-rotating
Motor power	1 kW
Speed range	1 to 350 rpm with 1 rpm precision

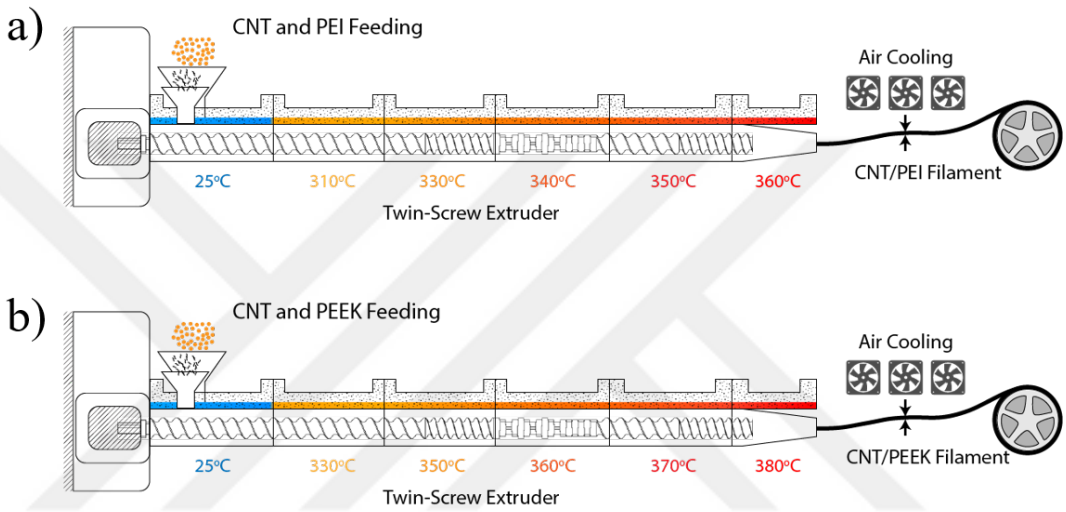

Figure 2.4 : Extrusion process of CNT reinforced (a) PEI and (b) PEEK.

Table 2.2 : Fabrication parameters of the composites.

Parameters	PEI	PEEK
Zone 1 (°C)	310	330
Zone 2 (°C)	330	350
Zone 3 (°C)	340	360
Zone 4 (°C)	350	370
Adapter (°C)	360	380
Screw Rotor Speed (rpm)	210	210

The fabrication of polymer nanocomposites from both PEI and PEEK matrices, the compression molding was performed by a hot press. Since the viscoelastic properties of CNT/PEI and CNT/PEEK composites are of interest, DMA samples were initially produced by using an aluminum mold. Before processing, all the neat polymer and CNT-reinforced PEI and PEEK granules were conditioned at 150°C overnight,

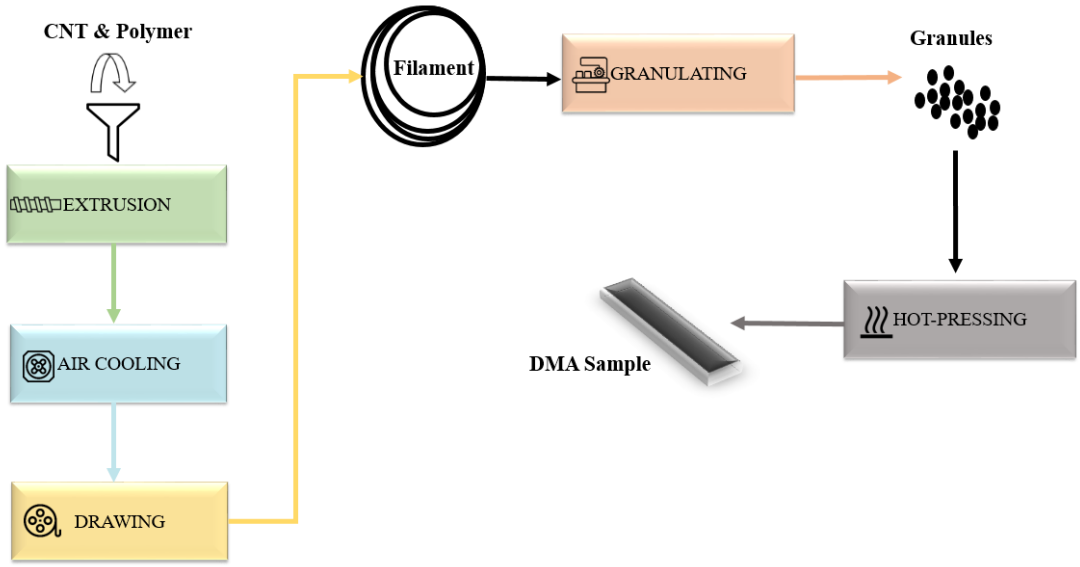

Figure 2.5 : Flow chart of composite fabrication.

removing water molecules to obtain a void-free structure. Production took place by applying 2.5 MPa pressure to the aluminum mold of 150x75x3 mm at temperatures between 300-330°C in about half an hour. Then the samples were cut to 65x13x3 mm with a conical tip on a three-axis CNC machine as required within the ASTM standard (see Fig. 2.6).

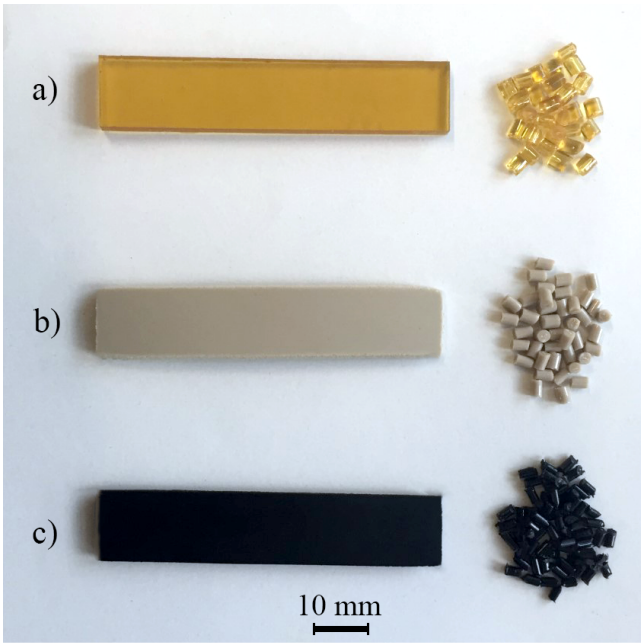

Figure 2.6 : DMA samples of (a) neat PEI, (b) neat PEEK, and (c) CNT reinforced composites.

2.3 Characterization

2.3.1 Thermogravimetric analysis (TGA)

Thermogravimetric analysis is a thermal analysis method in which the mass of a sample is monitored as a function of temperature and time under a controlled environment and temperature procedure. It provides both qualitative and quantitative information. With this method, it is possible to determine the thermal stability and decomposition temperature, as well as to moisture content, purity and compositions of the material.

In this study, thermal stability and decomposition temperatures of the neat PEI, PEEK and their CNT reinforced composites, weighing 10-12 mg, were examined by using TA Instrument-TGA55 at a heating rate of 10°C/min and the temperature range of 30-800°C under the nitrogen atmosphere (Fig. 2.7).

Figure 2.7 : TA Instrument-TGA55.

2.3.2 Differential scanning calorimetry analysis (DSC)

Differential scanning calorimetry (DSC) technique is used to investigate the physical and chemical change of polymers as a response to heating. It enables to quantitative and qualitative information about the material. It determines melting, crystallization, and glass transition temperatures, and the corresponding enthalpy and entropy changes, and changes in heat capacity or latent heat.

DSC measurements were performed in TA Instrument DSC Q2000 thermal analyzer in accordance with ASTM D3418-15 standards. Neat PEI and its composites, weighing 10-12 mg, were heated from 50°C to 350°C with a heating rate of 10°C/min to erase the

thermal history of the samples, then they were rapid cooled down from 350°C to 50°C and reheated up to 350°C with 10°C/min. All steps were carried out under nitrogen atmosphere. The same test procedure was performed for PEEK and its composites with an upper temperature limit of 400°C. Second cycle data were used in the analysis.

2.3.3 Scanning electron microscopy analysis (SEM)

Scanning electron microscopy analysis (SEM) is a visualisation technique that creates high magnified images of the sample by scanning it with a focused beam of electrons. In the SEM device, which consists of an electron gun, anode, magnetic lens, scanning coil, objective lens, detector, the electrons produced are sent to the sample and the detector captures the images. The interactions of the electrons with the sample are different, so images can be obtained from the secondary electron or the backscattering electron. SEM provides characterization of the materials by imaging the morphology of the sample surface, particle size, aggregated fillers and thickness of the filler material.

Morphology of the all samples were investigated by using Field Emission Scanning Electron Microscope (FE-SEM) (Quanta FEG 450), operating at 15 keV. To observe the dispersion and distribution of the fillers in the polymer matrix, the fractured cross-sectional area was obtained under cryogenic atmosphere, then coated with gold-palladium alloys.

2.3.4 Oscillation rheological analysis

Rheology analysis, which is related to the flow and deformation properties of the material, plays an important role in elucidating the physical and chemical structure of the material, so it has a great importance for the development of new materials and process improvements.

Dynamic rheological analysis was performed by a TA Discovery HR-2 rheometer using an aluminum parallel plate having 25 mm in diameter with 1 mm gap (Fig. 2.8). . Before the testing, all samples were conditioned in an oven at 150°C overnight. Firstly, strain sweep test was performed to determine the linear viscoelastic region in the strain (%) range between 0.0125 and 12.5 at angular frequency of 10 rad/s and at the temperature of 360°C. After deciding on the critical strain value for all samples,

frequency sweep test was carried out in an angular frequency range between 0.1 and 628 rad/s at 360°C.

Figure 2.8 : TA Discovery HR-2 rheometer.

2.3.5 Dynamic-mechanical analysis (DMA)

Dynamic mechanical analysis (DMA) characterize the viscoelastic behaviour of neat and filled polymers by being subjected to dynamic or cyclic forces. Depending on the shape of polymer materials, different deformation tools of the device such as tension, compression, 3-point bending, can be used which are functional according to measurement purposes.

Dynamic mechanical analysis (DMA) was performed on the all samples having approximately 65 mm in length, 13 mm in width, and 3 mm in thickness using a 35 mm dual cantilever in TA Instrument DMA 850in accordance with ASTM D5023 – 15 (Fig. 2.9). Before the testing, all samples were dried in an oven at 150°C overnight. First of all, an oscillation-strain sweep test was carried out to determine the linear viscoelastic region in the amplitude range between 0.1 and 50 μm at 35°C . Then, a temperature sweep test was performed at 1 Hz., in the range between 50 and 230°C at a heating rate 2°C/min.

2.3.6 Heat deflection temperature (HDT) testing

Heat deflection temperature (HDT) is a measure of the material's resistance to deflection under a certain stress at high temperature. The high HDT simplifies the

Figure 2.9 : TA Instrument DMA 850.

injection process, while improving the performance of the material in service. HDT is usually determined by the HDT-Vicat test, but it is also possible to determine HDT using the DMA device. In the test, a constant stress of 0.455 MPa or 1.82 MPa is selected and the point at which the sample subjected to temperature scanning under constant stress yields 0.25 mm of deflection or 0.121% in strain is considered HDT.

All samples having 65x13x3 mm in dimension were tested to find heat deflection temperature (HDT) using a 50 mm three-point bending clamp in TA Instrument DMA 850 (Fig. 2.9). Before the testing, all samples were dried in an oven at 150°C overnight. The temperature at a strain value of 0.121% in the samples subjected to temperature scanning under constant stress of 0.455 MPa was defined as HDT.

2.3.7 Flexural testing

Flexural testing of polymer materials measures flexural strength, which is related to the force required to bend the material. The test helps determine the resistivity of material before permanent deformation and the tendency to break. Different tools, like either 3 or 4-point bending, may have been used according to the properties of the tested materials. 3-point bending has been applied for homogeneous material, while the four-point test is the most available choice for non-homogeneous materials.

Flexural tests were applied; all samples having 65x13x3 mm in dimension at ramp to 0.35 mm with 0.05 mm/min ramping rate using a 50 mm three-point bending clamp in TA Instrument DMA 850 (Fig. 2.9). Before the testing, all samples were dried in an oven at 150°C overnight. According to ISO 178, flexural modulus was calculated at strain (%) range between 0.05-0.25.

3. RESULTS AND DISCUSSION

3.1 Thermogravimetric Analysis of CNT/PEI and CNT/PEEK Composites

Thermal stability and thermal decomposition temperature of neat PEI, PEEK, and their CNT reinforced composites were analyzed with thermogravimetry by examining the effect of filler when an amorphous (PEI) and semi-crystalline polymers (PEEK) were studied.

For PEI, as an aromatic polyimide, the chemical structure consists of repeating aromatic imide, propylidene (isopropylidene) and ether groups. The aromatic imide groups represents the stiffness and thermal resistance of the polymer, and the ether groups provide ease on the processibility with low melt viscosities. Although PEI is stable at high temperatures, with long dwell times in processes for advanced applications such in aerospace, medical, and electronics; thermal degradation needs to be further studied. Several earlier studies presented a two ways of thermal degradation of PEI through chain scission or crosslinking. In here, until 400 °C, neat PEI was thermally stable due to its phthalimide rings in its repeating units. A main decomposition step was observed approximately at 529 °C followed by the second step at 564 °C (Fig. 3.1). The first stage can be attributed to the scissioning of ether bridges and broken imide rings, while the second stage was about the stronger aromatic group [31, 70].

The addition of CNTs as 1, 3 and 5 wt.% showed a slight increase on the thermal stability of CNT/PEI composites. The onset degradation temperature, T_{onset}%, for neat PEI and 1, 3, 5 wt.% CNT/PEI composites were found as 515 °C, 520 °C, 519 °C, and 520 °C, respectively in an inert atmosphere (see Fig. 3.2 and Table 3.1). The maximum weight loss rate temperature (T_{max}%) for neat PEI was around 530 °C, whereas that of CNT reinforced composites increased by 3 °C to 533 °C (see Fig. 3.3 and Table 3.1). Also, at temperatures with 5% losses by weight (represented as T_5%) increased by 6 °C in all CNT reinforced PEI composites.

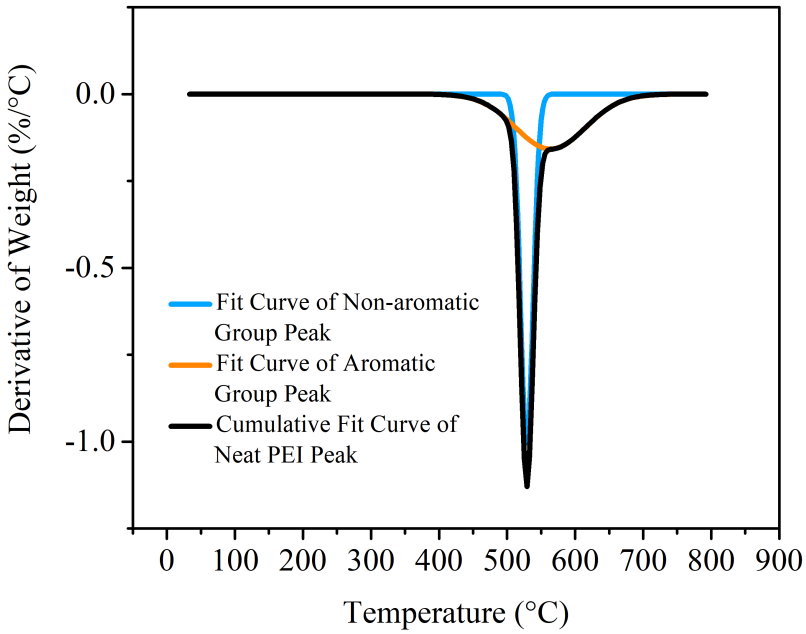

Figure 3.1 : TGA results of neat PEI focus on two stage decomposition.

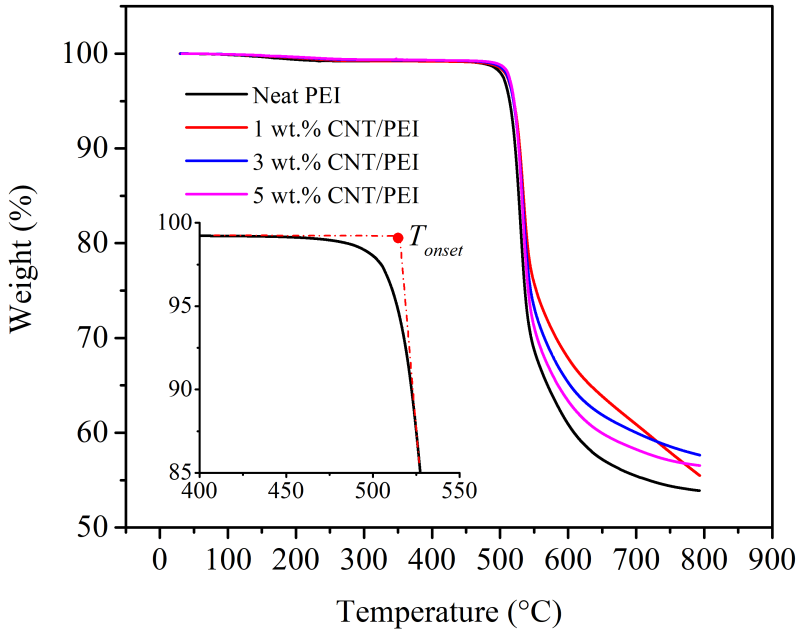

Figure 3.2 : TGA results of CNT/PEI composites focus on T_{onset}%.

PEEK is an aromatic polyketone combining ketone and aromatic moieties and the excellent thermal stability is achieved due to the stability of aromatic backbone. The weakest bond in bridging aromatic rings tend to start the random scissioning resulting with a noteworthy thermal stability over 565 °C [71, 72]. In an inert atmosphere

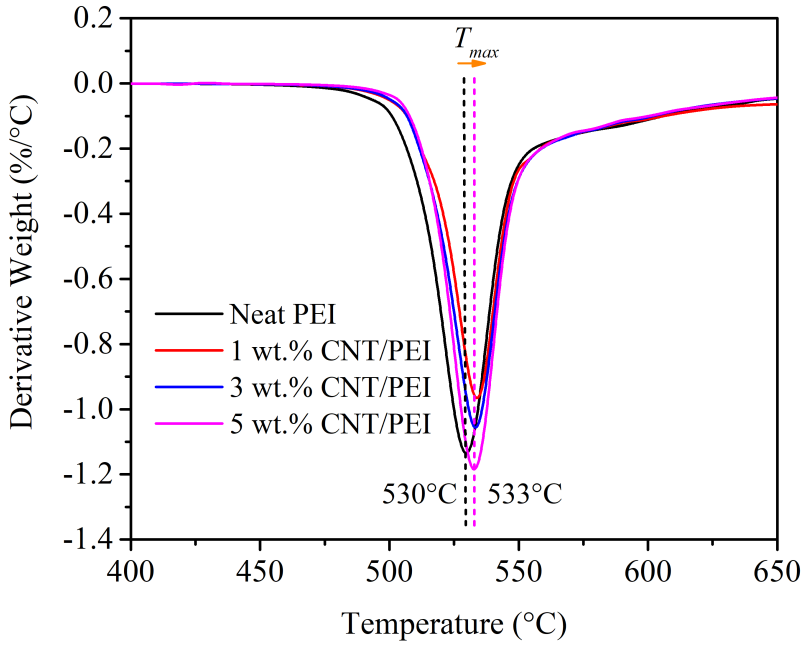

Figure 3.3 : TGA results of CNT/PEI composites focus on T_{max}%.

Table 3.1 : TGA results of CNT/PEI composites.

Polymer Type	CNT content (wt.%)	T_{onset} (°C)	T_5% (°C)	T_{max}% (°C)
PEI	0	515	514	530
	1	520	520	533
	3	519	520	533
	5	520	520	533

at a single stage, the degradation of PEEK and its composites contain dehydration, decarboxylation, and finally decarbonylation processes resulting with water, CO, CO_2, and phenols (Fig. 3.4).

For neat PEEK and 1, 3, 5 wt.% CNT/PEEK composites, T_{onset} was measured as 564 °C, 561 °C, 559 °C, and 560 °C, respectively in an inert atmosphere (see Fig. 3.5 and Table 3.2). The rapid weight loss that occurs below around 600 °C is mainly attributed to the phenols decomposition from PEEK with around 50 wt.%. T_{max}% was found 579 °C for neat PEEK, however, with the reinforcement of CNT, it decreased to around 575 °C (see Fig. 3.6 and Table 3.2).

Although slightly, the addition of 5 wt.% CNT to PEI and PEEK resulted contrary through increasing the T_{onset} of PEI by 5 °C, whereas decreasing the T_{onset} by 5 °C

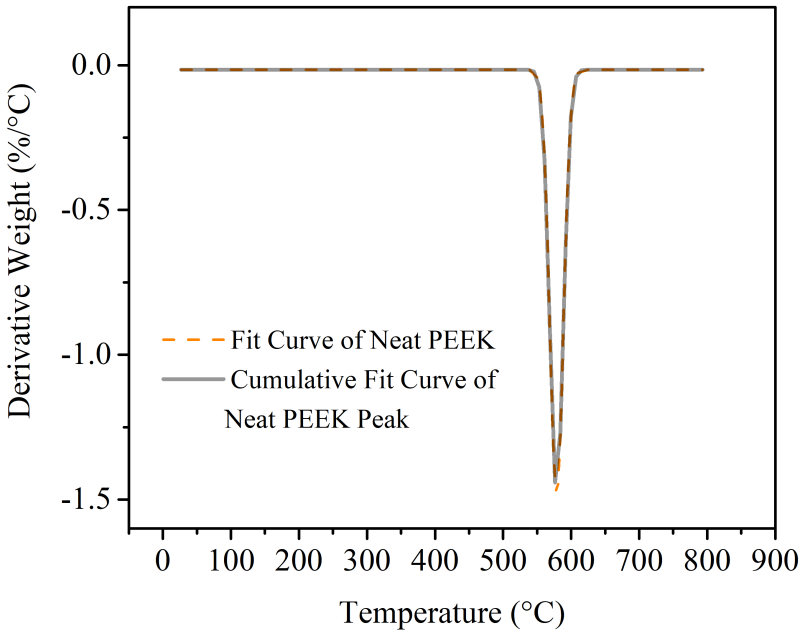

Figure 3.4 : TGA results of neat PEEK focus on one stage decomposition.

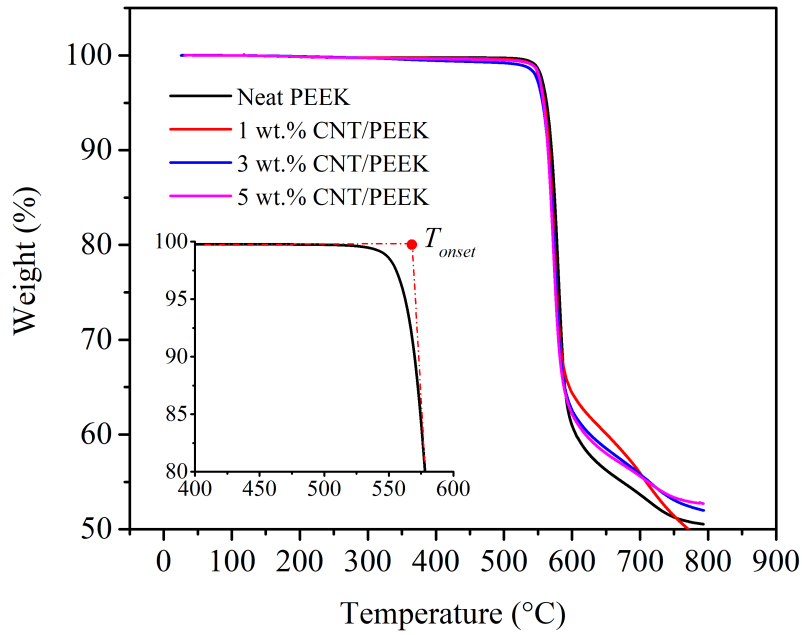

Figure 3.5 : TGA results of CNT/PEEK composites focus on T_{onset}.

in PEEK. This behavior demonstrated that CNT showed a barrier effect in the neat PEI, but it dissipated the thermal energy in the neat PEEK due to higher thermal conductivity arisen from its semi-crystalline chain morphologies [73]. Since the concentration of the CNT needs to be at a critical range for achieving an increased

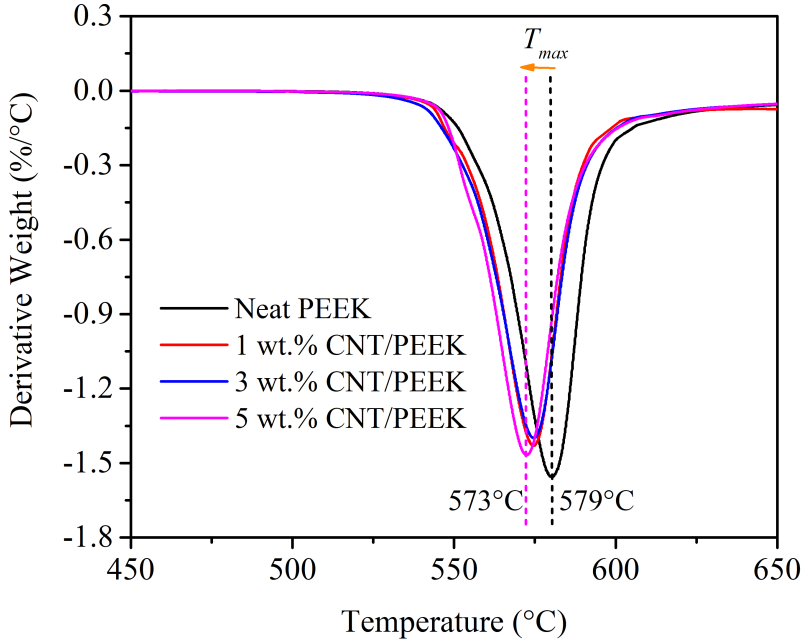

Figure 3.6 : TGA results of CNT/PEEK composites focus on T_{max}.

Table 3.2 : TGA results of CNT/PEEK composites.

Polymer Type	CNT content (wt.%)	T_{onset} (°C)	T_5% (°C)	T_{max}% (°C)
PEEK	0	564	561	579
	1	561	559	575
	3	559	559	575
	5	560	560	573

thermal decomposition temperature, none of the reported values can be related to this threshold to create such a drastic effect [74]. Overall the addition of CNT to PEI and PEEK did not cause a significant change in the thermal stability of these polymers, likewise in related studies [75]. Since all ether, and aromatic groups remain as residues till high temperatures, at 800 °C the residual weight was higher 54% for PEI and their composites and around 50% for PEEK and their composites as consistent with earlier studies (see Fig. 3.2 and Fig. 3.5) [71, 76].

3.2 Differential Calorimetry Analysis of CNT/PEI and CNT/PEEK Composites

The thermal transitions of high-performance thermoplastics is of great interest since these materials are alternatives to already existing thermoset based composites. But the high temperature processing conditions requires a significant characterization on

their phase transitions at particular temperatures. Since the degree of crystallinity is a positive factor in the mechanical characteristics, the addition of fillers such as CNTs should be studied in detail for the mobility of chains in polymers. Tracing the effect of CNT on the melt states of engineering thermoplastic polymer nanocomposites will bring benefits for developing advanced applications with multifunctionality. Hence, transitions driven by new domains like in CNTs is being investigated broadly for direct filler effects such as loading and aspect ratio. However indirect effects such as crystallinity on the thermal transitions, and rigid amorphous transitions (RAF) are less pronounced and discussed among the chain morphologies of the polymers such as PEI and PEEK. It is clearly known that CNT can promote specific semicrystalline morphologies or impose the ordering of polymers on the CNT surfaces [77, 78]. Establishing the relation in between these indirect effects on the overall properties of polymer nanocomposites is crucial to a deep understanding when various polymer types are considered.

The interfacial interaction in between the polymer and filler plays a significant role on the enhancement of the polymer nanocomposites due to the lower mobility of the polymer at this region compared to bulk fraction. Therefore, the interfacial polymer is described as immobile and RAF has been utilized for further discussions.

In here, DSC was performed to clarify the effect of CNT incorporation on T_g of neat PEI and PEEK, also the melting and crystallization behavior of neat PEEK.For thermograms, T_g manifests itself as a step and the temperature in the middle point of the slanted area (step) of the DSC plot (see Fig. 3.7). T_g was found as 216 °C and 152 °C for neat PEI and PEEK, while it was found as 218 °C and 152 °C for 5 wt.% CNT reinforced PEI and PEEK, respectively (see in Table 3.3). It was demonstrated that the presence of CNT did not significantly affect T_g of the polymers, as in similar nanocomposite studies [31, 79]. The reason for this phenomenon can be attributed to the weak filler-polymer interaction due to poor wetting and low adhesion of the CNT without any functional groups [80].

On the other hand, the melting temperatures (T_m) from the endothermic reaction in the DSC curve of neat PEEK and CNT/PEEK composites were around 341 °C (see Fig. 3.8). The result clearly presents that CNT addition did not show a drastic change on the melting temperature of PEEK, similar to earlier studies [79]. In addition, cold

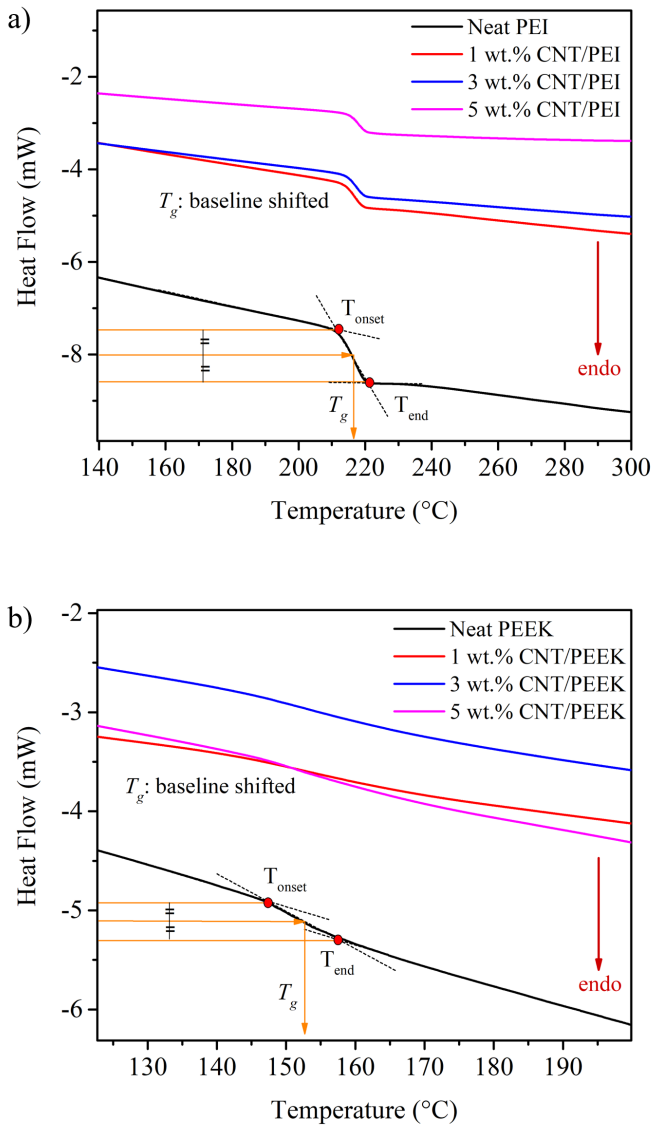

Figure 3.7 : DSC thermograms of (a) CNT/PEI composites and (b) CNT/PEEK composites focus on the glass transition regions.

crystallization, defined as an exothermic crystallization process observed between (T_g) and (T_m) temperatures, was not seen in PEEK samples due to the lack of mobile polymer chains to form a regular structure. However, hot crystallization temperature (T_{hc}), which was observed during cooling processing, was found between 258 °C and 266 °C and (T_{hc}) increased with the presence of CNT (see Fig. 3.9).

Moreover, crystallinity measurements of semi-crystalline PEEK samples were performed by utilizing Eq. 3.1. Heat fusion enthalpy of 100% crystalline PEEK (ΔH) was accepted as 130 J/g and $\Delta H_{measured}$ was calculated from integral of the area under melting peak being endotherm curve (see Fig. 3.10) [81].

Table 3.3 : T_g results of neat PEI, PEEK and their CNT reinforced composites.

CNT content (wt. %)	T_g of PEI samples (°C)	T_g of PEEK samples (°C)
0	216	152
1	217	154
3	217	153
5	218	152

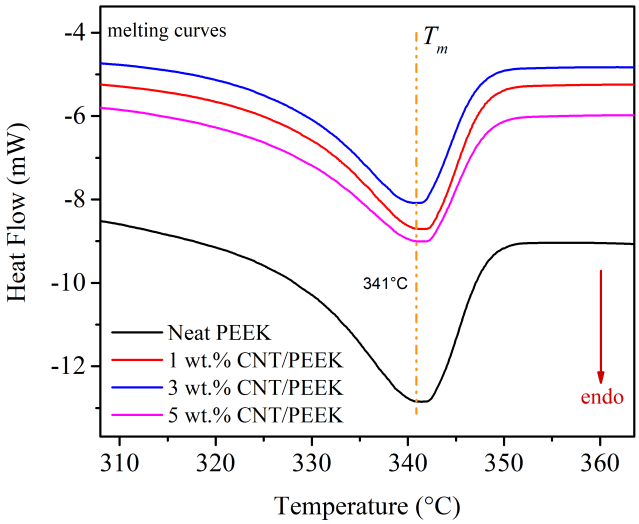

Figure 3.8 : DSC thermograms of CNT/PEEK composites focus on the melting regions.

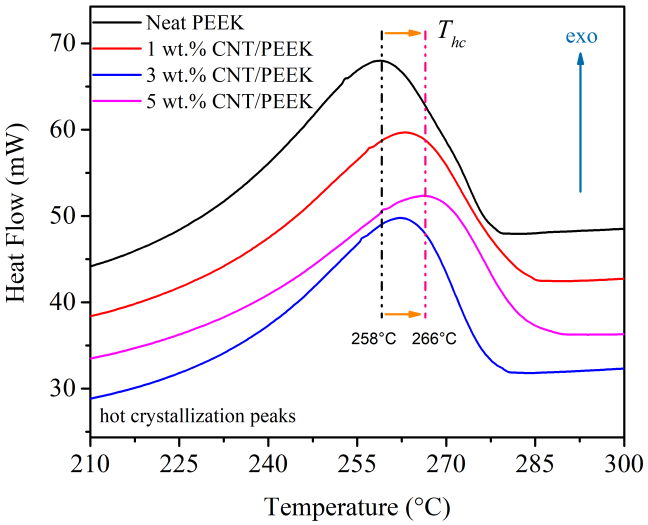

Figure 3.9 : DSC thermograms of CNT/PEEK composites focus on hot crystallization.

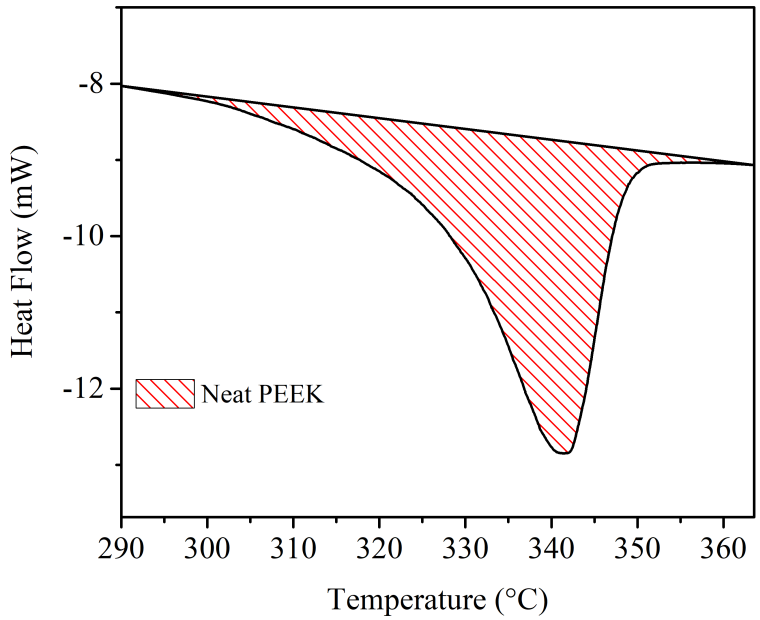

Figure 3.10 : DSC thermograms of neat PEEK focus on calculation of the heat fusion entalpy.

$$X_{CF} = \frac{\Delta H_{measured}}{\Delta H} \tag{3.1}$$

Also, ternary phase systems including crystalline (CF), rigid amorphous (RAF), and a mobile amorphous fraction (MAF) for semi-crystalline polymers were studied in detail. Amorphous zones referred as mobile and rigid is the main difference in a ternary and binary phase system. RAF is defined by the region of restricted mobility around the crystalline domains and does not contribute T_g, just like the crystalline fraction, but MAF relaxes and contributes to a heat capacity changes at Tg [81]. MAF and RAF were estimated using Eq. 3.2 and Eq. 3.3. In the equations, ΔC_p and ΔC_p^{α} represent specific heat capacity change of the sample and specific heat capacity change of 100% amorphous PEEK at T_g, respectively. Tangents were plotted to $C_{p,solid}$ and $C_{p,liquid}$ in Fig. 3.11, then the ΔC_p change at the midpoint (T_g) of the transient region was calculated and ΔC_p^{α} was taken as 0.27 J/g°C according to Advanced Thermal Analysis System data bank [81].

$$X_{MAF} = \frac{\Delta C_p}{\Delta C_P{}^a} \times 100\% \tag{3.2}$$

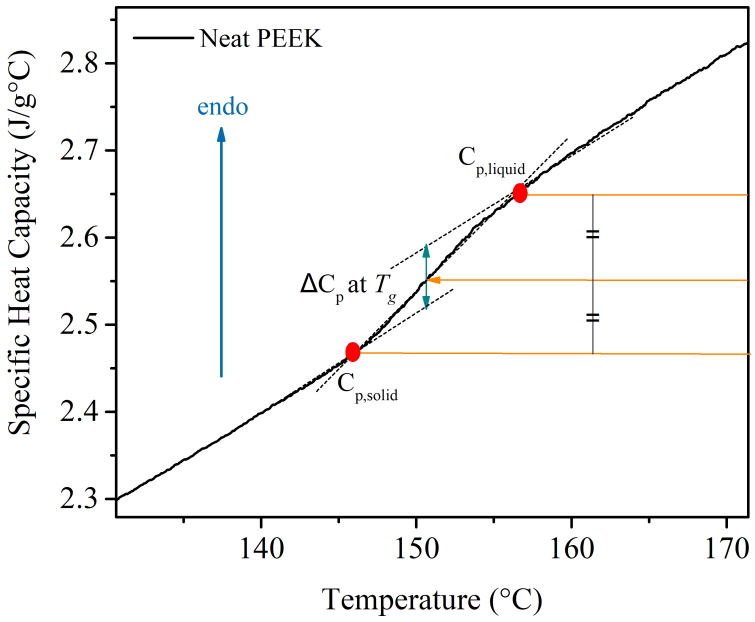

Figure 3.11 : DSC thermograms of CNT/PEEK composites focus calculation of ΔC_p at T_g.

$$X_{RAF} = 1 - X_{CF} - X_{MAF} \tag{3.3}$$

It should be clarified that the RAF is formed not only by the restricted amorphous polymer chains around the crystalline region, but also the chains with restricted mobility originating from the reinforcement material [82]. However, it was not possible to calculate these two fractions with only DSC analysis, so the calculated RAF was the sum of the restricted area due to the crystal region and the contribution of CNT [82]. Based on the ternary phase system, neat PEEK and CNT/PEEK composites were schematized in see Fig. 3.12 and all results were tabulated in Table 3.4.

Table 3.4 : DSC results of neat PEEK and their CNT reinforced composites.

Sample Name	T_m (°C)	T_{hc} (°C)	$\Delta H_{measured}$ (J/g)	$\%X_{CF}$	$\%X_{MAF}$	$\%X_{RAF}$
Neat PEEK	341	258	34	26	39	35
1 wt.%CNT/PEEK	341	263	38	29	32	39
3 wt.%CNT/PEEK	341	262	34	27	32	41
5 wt.%CNT/PEEK	341	266	35	27	28	44

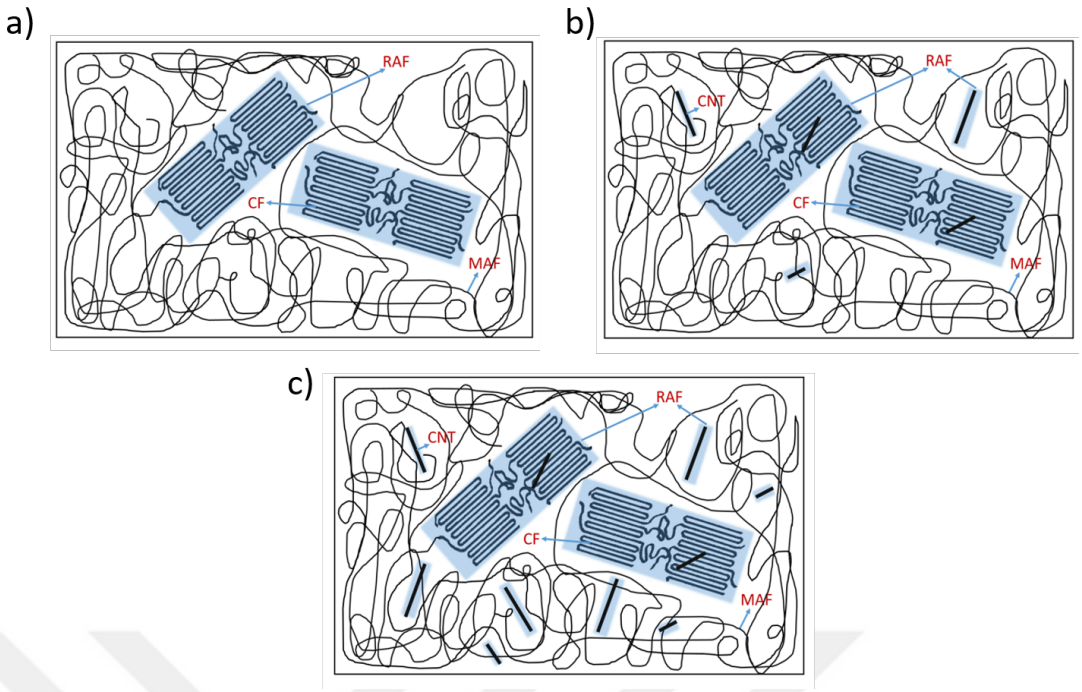

Figure 3.12 : Representation of the ternary phase system for (a) Neat PEEK, (b) 1 wt.% CNT/PEEK, and (c) 5 wt.% CNT/PEEK.

In earlier studies, the addition of CNT in a PEEK composite resulted with increased crystallinity and the reason for such findings were attributed to the presence of CNTs as if triggering the nucleation and forcing an ordered fashion [60]. In addition, as stated before, the increase of T_{hc} with the amount of CNT was a sign of heterogeneous nucleated sites, like other CNT/PEEK studies [83]. Also, the highest crystallinity was obtained from 1 wt.% CNT/PEEK composite as 29% while neat PEEK had 26%. CNT decreased the amount of MAF in PEEK both by increasing the crystal ratio and by embedding in amorphous regions, limiting the mobility of polymer chains. The value of RAF for neat PEI 35% while that of CNT/PEEK composites varied between 39% and 44% (see in Table 3.4). RAF showed an increasing trend with respect to the amount of CNT and highest RAF was obtained from 5 wt.% CNT/PEEK composite, due to an increase in crystalline fraction and restricted area by the CNT. Although the crystal ratio is the highest in the 1 wt.% CNT/PEEK composite, it is thought that CNT are mostly embedded in the crystalline regions, since the RAF ratio is the lowest. When the amount of CNT increased from 1 to 3 and 5 wt.%, it was accepted that CNT was more distributed in amorphous chains, and thus, chain mobility was inhibited and RAF increased (see Fig. 3.12 (b) and Fig. 3.12 (c)).

3.3 Morphological Analysis of CNT/PEI and CNT/PEEK Composites

The structural characteristics of the CNTs play a significant role in determining its properties and the properties of the composite material as a whole. The morphology of CNT/PEI and CNT/PEEK systems was examined employing the SEM method. The cryo-fractured composites were investigated to establish the relationship between the structure and property of the all polymer nanocomposites. The SEM images of the fabricated CNT/PEI composites are shown in (see Fig. 3.13). Without any functionalization or surface treatment of CNT, good quality of dispersion and distribution of polymer nanocomposites were achieved by melt-processing where shear forces dominating the overall process as depicted in Fig. 3.13. Along with the good dispersion of CNT, the polymer bridging was also observed when compared with neat PEI. The increase in CNT ratio also resulted with more fibrillary formation in a PEI matrix similar to many thermoplastics as presented in see Fig. 3.13 from 1 to 5% wt. of CNT [31]. To investigate the morphology in more details, SEM images were taken for each CNT/PEI sample at 80.000X magnifications (see Fig. 3.13). The white dots and lines indicated the CNT, while the darker parts were the PEI matrix itself, pointing out that CNT were well covered by the matrix and no pull-out mechanism was observed during cryo-fracturing of the specimens. In here, hot press was employed as a composite manufacturing process in which especially at very high T_g polymers such as PEI, the process may result with drawbacks such as causing irregularities such as voids. Hence, the presence of voids at higher CNT fractions was also attributed to the higher viscosities of the polymer at these loadings limiting the melt flow and resulting with flaws as presented in Fig. 3.13 (c).

The cryo-fractured SEM results of neat PEEK and CNT/PEEK composites were presented in Fig. 3.14 at 80.000X as similar to CNT/PEI with white dots and lines representing the CNT, while the darker parts were the matrix. Melt processing of CNT reinforced PEEK composites also showed a well dispersed and distributed polymer composite by overcoming the electrostatic interaction and van der Waals force between CNT with the help of the high shear force coming from extrusion, as in PEI (see insert images in Fig. 3.14). When the CNT filler content is increased from 1 to 5 wt.%, less irregularities such as voids was observed compared to 5 wt.% CNT/PEI composites. One particular reason for that may be attributed to the lower T_g of PEEK compared to

PEI and also lower phonon scattering due to crystalline domains of PEEK that creates a more homogeneous thermal pathway [73].

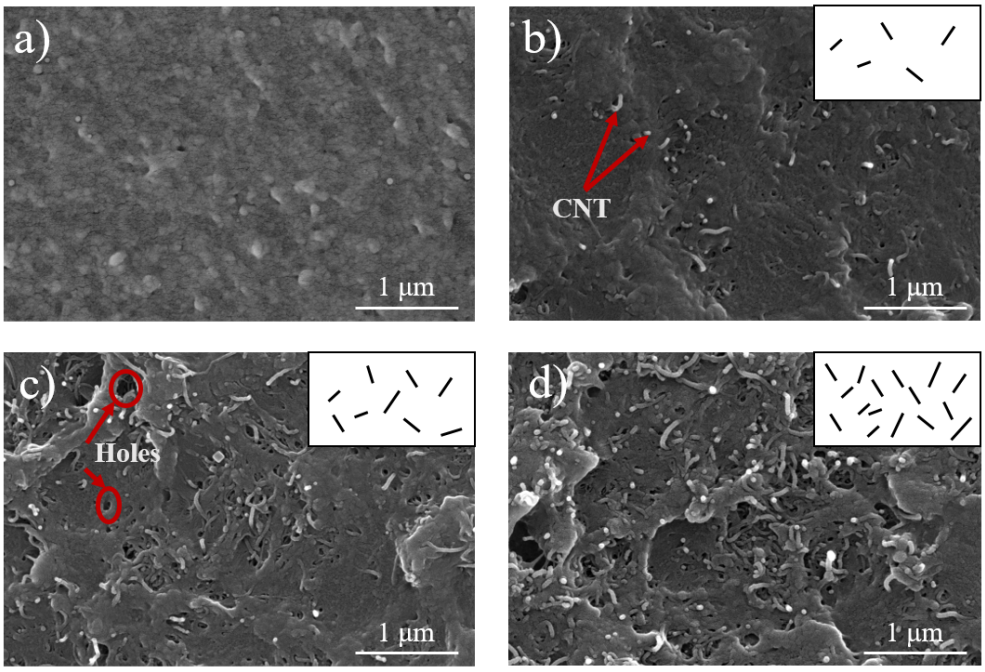

Figure 3.13 : Morphological results of (a) neat PEI, (b) 1 wt.% CNT/PEI, (c) 3 wt.% CNT/PEI, and (d) 5 wt.% CNT/PEI images (Insert images represent the distribution level as regards the CNT amounts.).

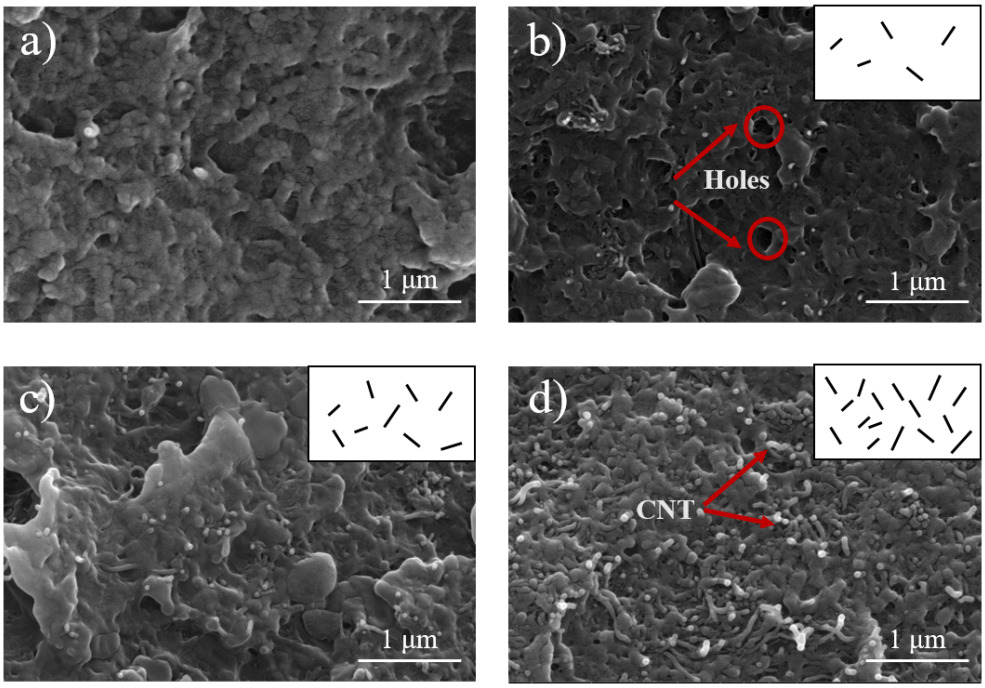

Figure 3.14 : Morphological results of (a) neat PEEK, (b) 1 wt.% CNT/ PEEK, (c) 3 wt.% CNT/ PEEK, and (d) 5 wt.% CNT/ PEEK images (Insert images represent the distribution level as regards the CNT amounts.).

3.4 Oscillatory Rheology Analysis of CNT/PEI and CNT/PEEK Composites

3.4.1 Strain dependency of viscoelastic properties

The properties of polymer nanocomposites are strongly related to adequate dispersion of the fillers into the polymer matrix. Exploring the dispersion quality in the polymer nanocomposites is usually not straightforward since researchers may find answers either locally or globally at post factum with limited possibility for in-situ observations. However, rheological characterizations may offer the investigation of the liquid state with fillers since the linear and non-linear properties are sensitive to changes at the microstructural scale.

In this section, the strain dependence viscoelastic properties of neat PEI, PEEK, and their CNT reinforced composites were investigated. A strain sweep test was performed to identify linear viscoelastic region (LVR) and to reveal the effect of microstructure when fillers are present. In addition, critical strain values of CNT/PEI and CNT/PEEK composites were obtained since will be important to examine at the frequency dependent viscoelastic properties of them at linear region. The critical strain which is defined as the transition from linear to non-linear behavior was defined at a decrease in 5-10% for storage modulus [84]. Hence, it is important to define the critical strain to determine the transitions from linear to non-linear regimes where regions up to critical strain is LVR.

When neat PEI and PEEK considered, even at high strains a Newtonian plateau was observed presenting the absence of any solid network formation when fillers was not present [85]. Oppose to that, CNT/PEI and CNT/PEEK composites showed the non-linear behavior at high strains with a dramatic yielding at their critical strains (Fig. 3.15). Similar to studies from literature, at the critical strain values of all CNT/PEI and CNT/PEEK composites, a decrease of storage modulus was observed [84, 86–89]. This was attributed to the Payne effect, a phenomenon associated with the deterioration of the filler-filler network structure [85]. With an increasing filler content, the Payne effect is more pronounced and decreased the critical strains presenting a dense network in the matrix similarly in PEK, PC, ABS nanocomposites [90]. On the other hand, the

plateau modulus increased when CNT content was at 5 wt.% in both CNT/PEI and CNT/PEEK around 6E4% and 2E3%, respectively (see arrows in Fig. 3.15). The higher enhancement capability observed in CNT/PEI composites may be attributed to a better CNT-polymer interaction where amorphous chain structure is also effective for a high aspect ratio filler.

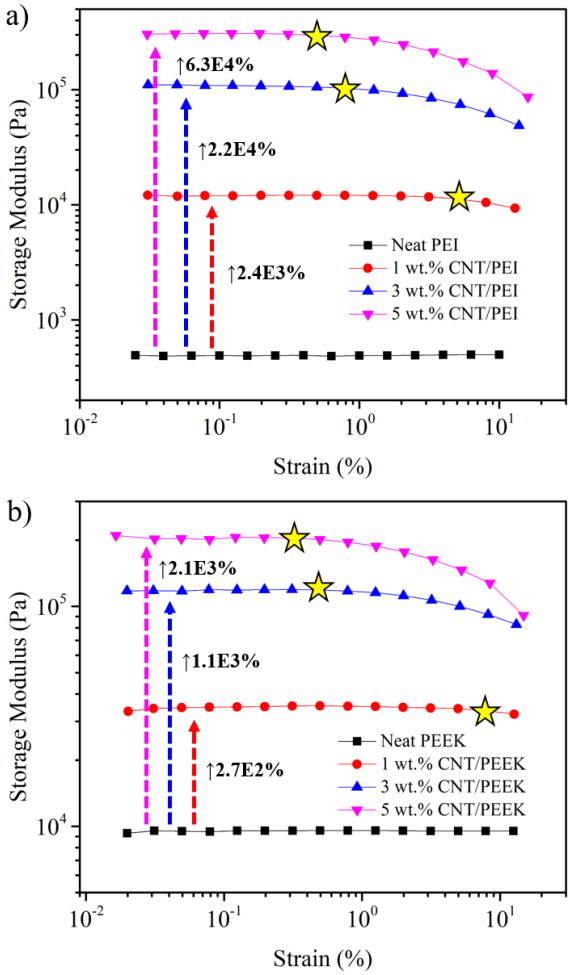

Figure 3.15 : Strain-storage modulus graph of neat and CNT reinforced (a) PEI (b) PEEK samples. %Increments in storage modulus and the critical strain values are represented as arrows and stars, respectively.

Additionally, an exponential dependence of the critical strains were observed to volume fraction of CNT ($\gamma_c \propto \theta_f^n$), which is represented with the Power Law similar to earlier studies [84, 91–93]. The Power-Law on the logarithmic scale showed the slopes for PEI and PEEK as -1.76 and -1.40, respectively (Fig. 3.16). The slope for CNT/PEI composites is higher than CNT/ PEEK composites and can be associated with CNT-polymer interaction and CNT-CNT network formation due to the efficiency

of dispersion and distribution [91, 92]. More detailed analysis of the interaction of CNT to PEI and PEEK was investigated in frequency-dependent properties.

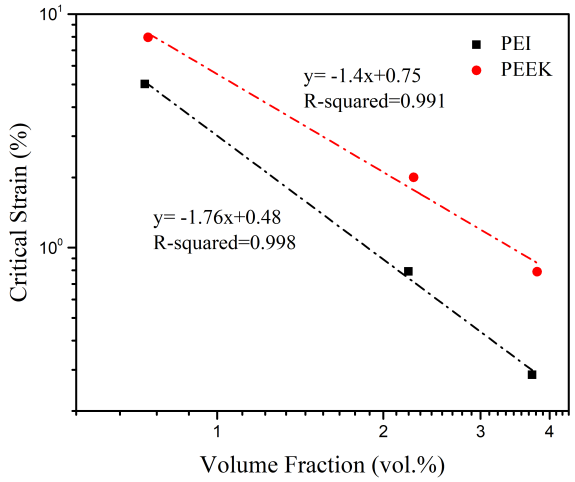

Figure 3.16 : Critical strain-volume fraction graph of PEI and PEEK samples.

3.4.2 Frequency dependency of viscoelastic properties

3.4.2.1 Analysis of storage modulus - frequency plots

The study of frequency-dependent behavior of reinforced polymer composites is critical from the scientific to industrial perspective to determine the process conditions when scale-up is considered [94]. At high frequencies, the results are usually evaluated to reveal the effect of filler on the overall processing properties. Besides, at lower frequencies the rheological results are usually sensitive to composite structure and gives information about the percolation state of the filler. In here, the frequency-depended behavior of the CNT reinforced PEI and PEEK composites was investigated in linear viscoelastic region (LVR). Although the storage module is sensitive to microstructural changes in the low-frequency regions (up to 1 rad/s), the high-frequency regions act oppositely. For CNT/PEI and CNT/PEEK composites, the storage modulus of all samples showed an increase with the increasing frequency, particularly in the high-frequency regions where the material is not allowed to flow for a long time (Fig. 3.17). Also, the storage modulus of neat polymers and CNT/PEI and CNT/PEEK composites showed a similar trend at high-frequency with the lack of required relaxation time for the polymer chains. And hence increasing frequency eliminated the effect of the CNT on the short-range dynamics of the polymer [94].

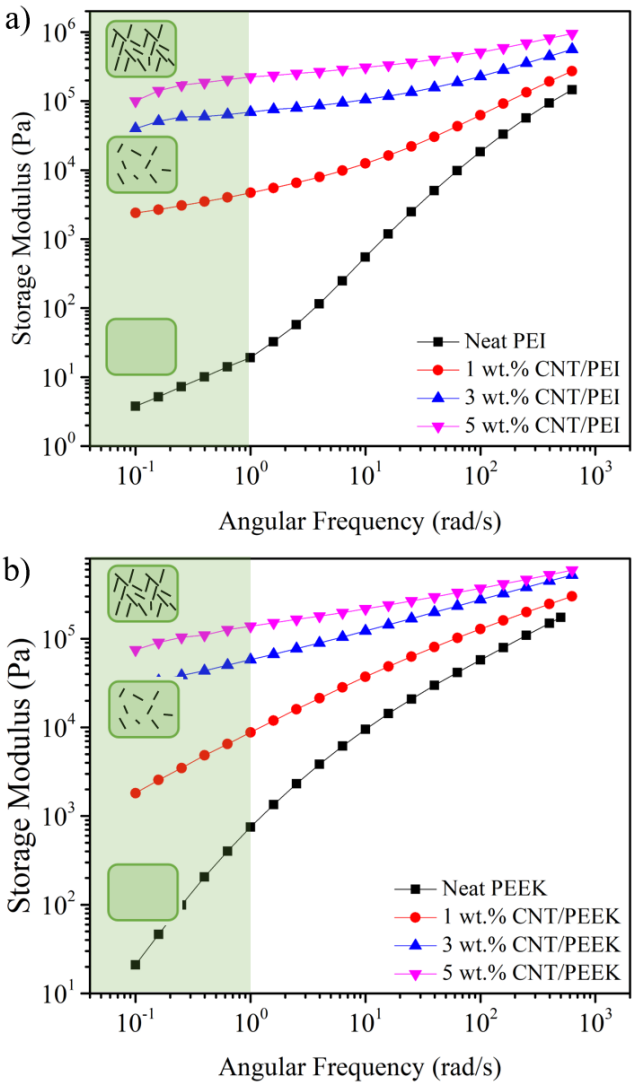

Figure 3.17 : Storage modulus as a function of frequency for (a) neat PEI and CNT/PEI and (b) neat PEEK and CNT/PEEK composites.

In the low-frequency regions, the fully relaxed PEI and PEEK are exponentially frequency-dependent. They are expected to exhibit typical terminal behavior by obeying $G' \propto \omega^2$ scaling, however, PEI and PEEK showed terminal behavior with 0.7 and 1.56 scaling, respectively, which may be related to the difference in the polydispersity of the polymers [95] (see Table 3.5). This frequency dependence is an indication of the predominance of a liquid-like structure in the system, consistent with previous findings for thermoplastics [27, 43]. On the other hand, the degree of frequency dependence began to disappear when CNTs present, which restricts polymer relaxations and indicate the dominant liquid to solid-like transition. This behavior is attributed to the rheological percolation where CNT-CNT interaction is

Table 3.5 : Frequency dependency exponent of neat PEI, PEEK and their CNT reinforced composites.

CNT content (wt.%)	Frequency-dependency exponent	
	PEI	PEEK
0	0.70	1.56
1	0.29	0.68
3	0.21	0.34
5	0.32	0.27

more pronounced [19] and a sudden increase in storage modulus is presented. The addition of CNTs increased the storage modules of neat PEI and PEEK by 6E4% and 8E3% (see (Fig. 3.18) [31, 43]. For CNT/PEI composites, a sharp increase was observed at 1 wt.% CNT where the slope was decreased by 58%, and frequency dependence disappeared, indicating that the percolation threshold was lower than 1 wt.%, in consistent with earlier findings [31]. Even, with 3 wt.% CNT reinforcement, the slope further decreased and reached the plateau region, which indicated the solid-like feature as dominant. Similar behavior has been observed in CNT/PEEK composites, and the percolation threshold was reported to be below 1 wt.% [39].

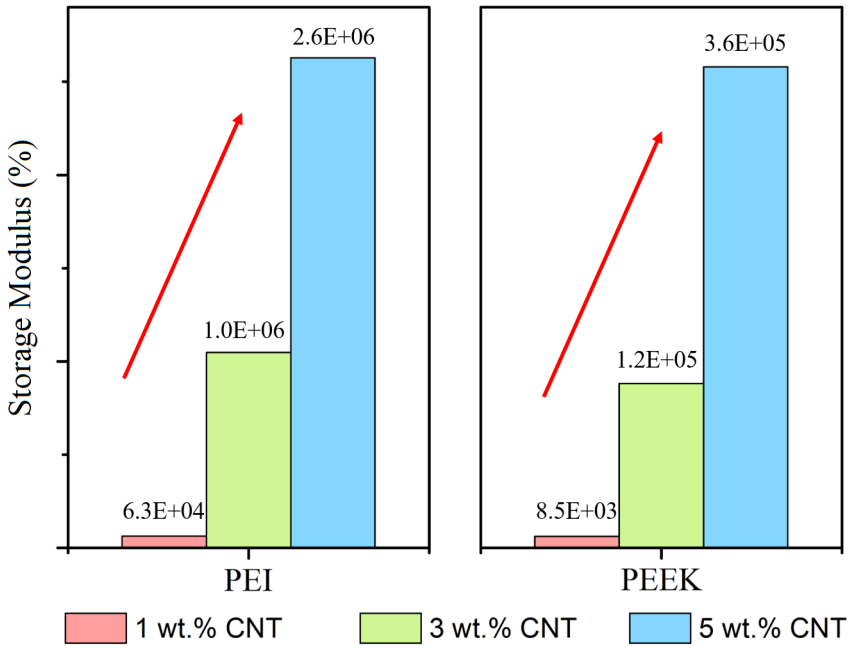

Figure 3.18 : The change in storage modulus for (a) CNT/PEI and (b) CNT/PEEK composites.

3.4.2.2 Analysis of complex viscosity-frequency plots

The complex viscosity, referred as the total resistance to flow was also studied to reveal the effects of CNT reinforcement for processing. From Fig. 3.19, the neat PEI and PEEK exhibited a typical thermoplastic behavior showing a Newtonian plateau at low frequency where the chain entanglements are present, and a shear-thinning at high frequency indicating the disentanglement of polymer chains during flow [96].

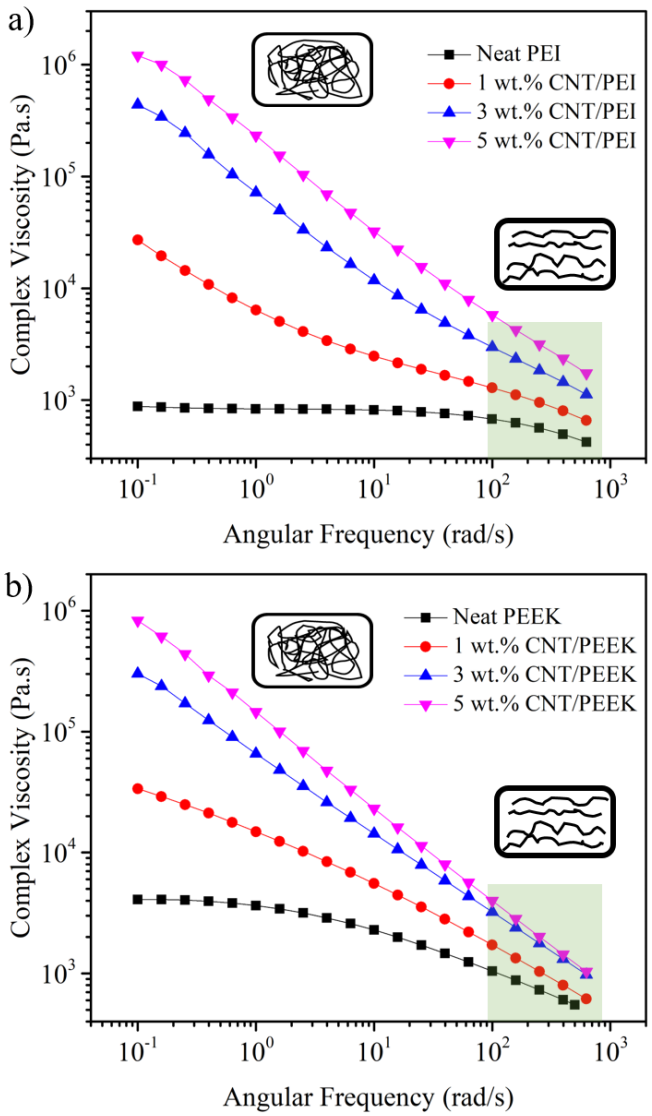

Figure 3.19 : Complex viscosity as a function of frequency for (a) neat PEI and CNT/PEI and (b) neat PEEK and CNT/PEEK composites.

At higher CNT loadings, the complex viscosity increased and shear thinning behavior was observed in all frequency ranges likewise similar nanoparticle reinforced composites [27,43]. This phenomenon can be illustrated with the Power Law equation

($C\dot{\gamma}^{(n-1)}$), n is defined as shear-thinning exponent) by utilizing the Cox-Merz rule ($\eta(\dot{\gamma})$=$\eta^*(\omega)$, for $\dot{\gamma} = \omega$) [90, 97]. It was observed that the n value of PEI and PEEK decreased with increasing CNT, and the lowest n was obtained from 5 wt.% CNT/PEI and 5 wt.% CNT/PEEK composites as 0.35 and 0.26, respectively at a frequency range between 10^2 and 10^3 rad/s (Table 3.6) meaning shear-thinning feature became more pronounced with CNT incorporation.

Table 3.6 : Shear-thinning exponent (n) of neat PEI, PEEK and their CNT reinforced composites.

CNT content (wt.%)	Shear-thinning exponent (n)	
	PEI	PEEK
0	0.72	0.60
1	0.64	0.45
3	0.47	0.35
5	0.35	0.26

The restrictions of chain movement was clearly presented when CNT content increased to 5 wt.% through the increased complex viscosity. Although from the processing requirements, an increase in complex viscosity is a disadvantage, the shear-thinning feature dominated [31]. Moreover, the sudden increase in the complex viscosity of PEI and PEEK and the transition of Newtonian behavior to shear thinning in the low-frequency region with CNT also indicated that the percolation threshold was below 1 wt.%.

3.4.2.3 Analysis of modified Cole-Cole plots

The modified Cole-Cole plots (or Han Plot) obtained by plotting the storage modulus versus the loss modulus is an analogy to dielectric spectroscopy made on polymer relaxations [24, 27]. It is an effective technique to analyze the structural change in polymers and to use revealing percolation threshold of the polymer composites [24,98].

Cole-Cole plots of PEI and PEEK samples were plotted on a logarithmic scale and in general, the Cole-Cole plots provide a master curve with a slope of 2for homogeneous polymer melts and the deviation in the slope is indicative of heterogeneity (Fig. 3.20) [99]. Evaluating the slope of the neat PEI and PEEK polymers was found

approximately 2, while the slope decreased rapidly with the CNT reinforcement, which is a sign of the structural change in the system. In addition, neat PEI and PEEK showed viscous properties in all frequency ranges (loss modulus is higher than storage modulus), in contrast, 3 wt.% and 5 wt.% CNT reinforced PEI and PEEK composites presented an elastic characteristics. chain characteristics of an amorphous to semi-crystalline domains. The percolation threshold described as below 1 wt.% for PEI and PEEK earlier was also confirmed with Cole-Cole plots.

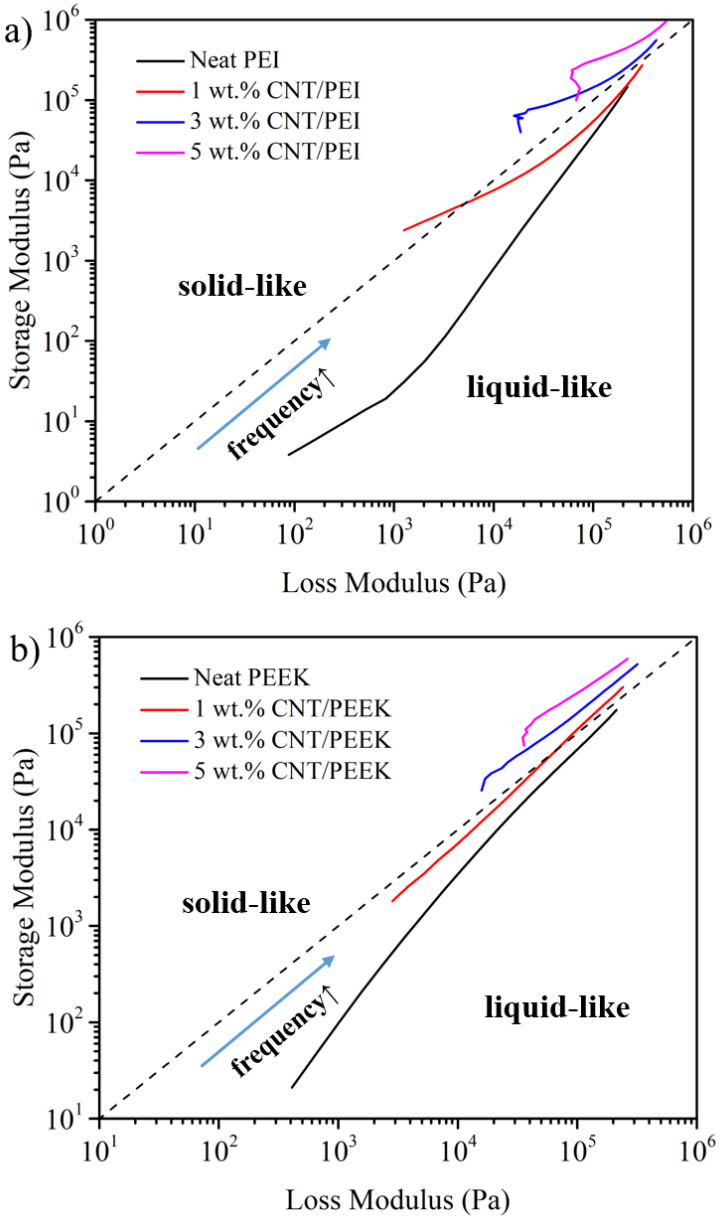

Figure 3.20 : Modified Cole-Cole graph for (a) neat PEI and CNT/PEI and (b) neat PEEK and CNT/PEEK composites.

3.5 Dynamic-Mechanical Analysis of CNT/PEI and CNT/PEEK Composites

DMA clarifies both the elastic and viscous response of the materials under cyclic deformation depending on the frequency. Also, DMA reveals both the potential in load-bearing applications of materials by analyzing the change in the storage modulus, representing the stiffness of the composite, and filler-polymer interaction by examining the tan delta value which is a sign of heat dissipation ability of the material. It is critical to analyze change in material behavior correspond to temperature to explore thermo-mechanical performance of the material, for this reason DMA is one of the effective characterization techniques to determine the glass transition region in the high sensitivity. In this section, the change in the thermo-mechanical properties of the polymers having a different structure with the addition of CNT was investigated.

DMA was performed on neat PEI, PEEK and CNT/PEI and CNT/PEEK composites. In DMA, two main regions were observed: the first one was a glassy region and the latter was a rubbery region (see Fig. 3.21). Storage modulus in the glassy region decreased with increasing temperature and the sudden change was observed at T_g for all samples, due to increasing molecular mobility of the polymers (Fig. 3.22) [100]. A sudden decrease in storage modulus was more drastic in PEI samples compared with PEEK ones, because the crystal region still provides stiffness, so the loss of stiffness was less in semi-crystalline PEEK samples [101].

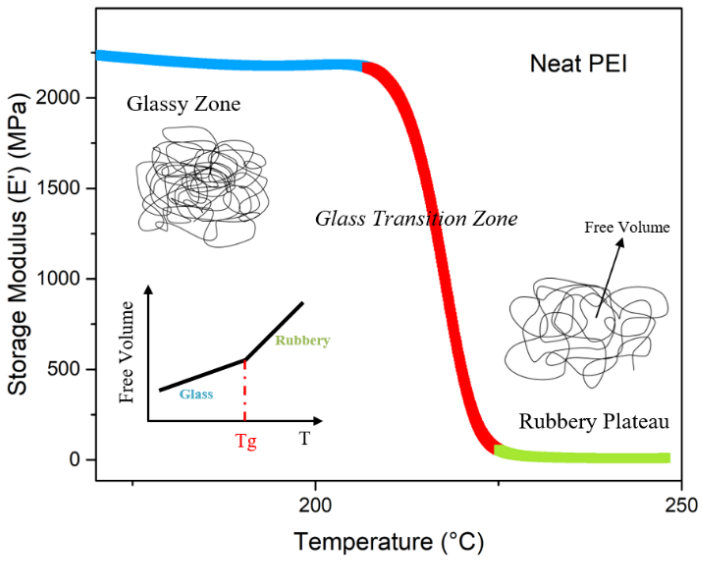

Figure 3.21 : Representation of the glassy and rubbery region.

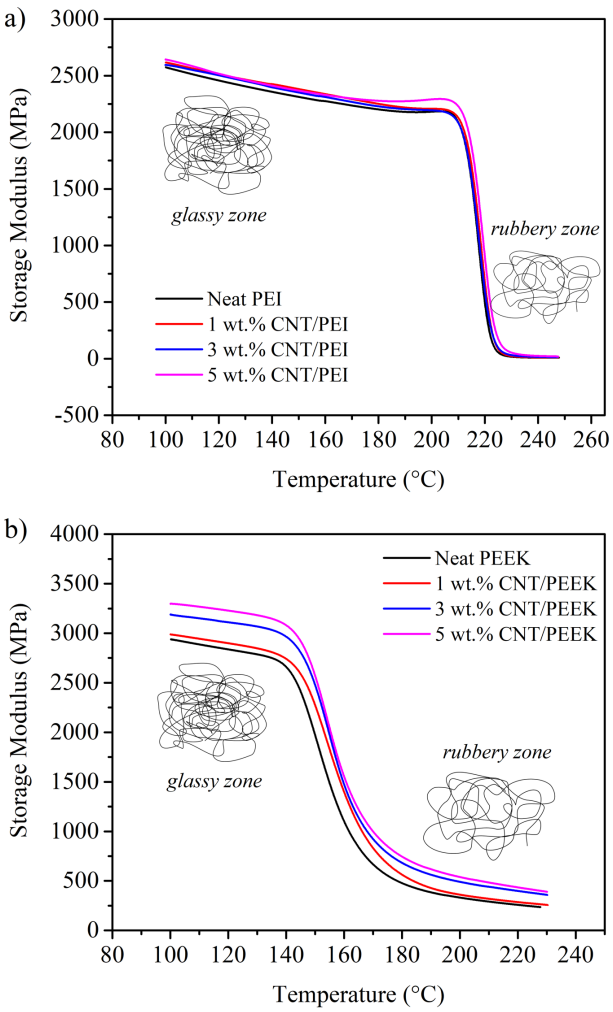

Figure 3.22 : Storage modulus as a function of temperature for (a) CNT/PEI and (b) CNT/PEEK composites.

For both CNT/PEI and CNT/PEEK composites, addition of CNT to these polymers showed an increase in the storage modulus in both the glassy and rubbery regions. The results may be attributed to a well CNT to polymer interaction and adhesion in which the highest achievement for the glassy region was with 5 wt.% CNT/PEI and PEEK composites [102,103]. However, when compared to an amorphous vs. semi-crystalline polymer, the enhancement capability was more significant in CNT/PEEK composites where CNT acted as nucleation sides for crystalline domains. Moreover, since the specimen fabrication was performed by hot-press rather than injection molding, the formation of voids in CNT/PEI composites was more significant with higher T_g leading to a lower mechanical characteristic. For tan delta, both CNT/PEI and CNT/PEEK composites had decreased the height and area suggesting the confinement of polymer

chains with CNT (Fig. 3.23) [30, 100]. Also, T_g of the CNT/PEI and CNT/PEEK composites were calculated from both the onset point of the storage modulus and the peak point of the tan delta curve (see Table 3.7) The findings were in line with the DSC analysis, confirming that the CNT did not significantly affect the T_g of the polymers.

Table 3.7 : T_g results of CNT/PEI and CNT/PEEK composites by DMA.

CNT content (wt.%)	T_g (°C) by Storage Modulus		T_g (°C) by Tan Delta	
	PEI	PEEK	PEI	PEEK
0	217	145	226	161
1	218	148	226	164
3	217	148	226	164
5	218	147	226	164

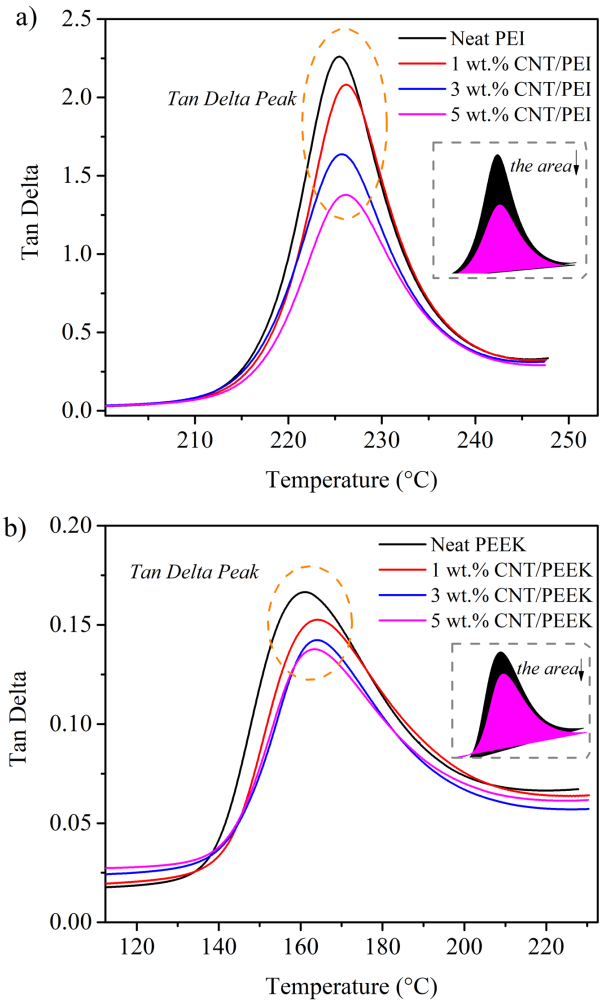

Figure 3.23 : Tan delta as a function of temperature for (a) CNT/PEI and (b) CNT/PEEK composites.

Since the polymer type plays a crucial role on the overall enhancement capability when a filler such as CNT is present, understanding the CNT-polymer and CNT-CNT interaction is important. Analytical approaches considering the amorphous or semi-crystalline nature of the polymers when reinforced with CNT is usually described upon the polymer chain movement. In here, the reinforcing efficiency of CNT in polymers with different structures, the change in the entanglement level in the polymer chain with the increasing amount of CNT, and the constrained region in polymers due to CNT were revealed.

Initially C factor which evaluates the efficiency of CNT in a polymer matrix for reinforcement is studied [21]. For all calculations, the storage modulus was used in between 170 °C and 230 °C for PEI, 130 °C and 200 °C for PEEK, at the glassy and rubbery regions, respectively (see Eq. 3.4).

$$\text{C factor } (C) = \frac{\left(E'_g/E'_r\right)_{\text{composite}}}{\left(E'_g/E'_r\right)_{\text{polymer}}} \tag{3.4}$$

It is well-known that as the C factor increases, the reinforcing effectiveness is expected to decrease [21, 33]. Along with the calculations, the C factor for CNT/PEI and CNT/PEEK was decreased with the CNT concentration (Fig. 3.24). The lowest C factor was calculated as 0.27 and 0.30 from 5 wt.% CNT/PEI and 5 wt.% CNT/PEEK composites, respectively. These results showed that 5 wt.% CNT had more efficiency in the distribution in the polymers, which was supported with the morphological characterization by SEM image given in section 3.3.

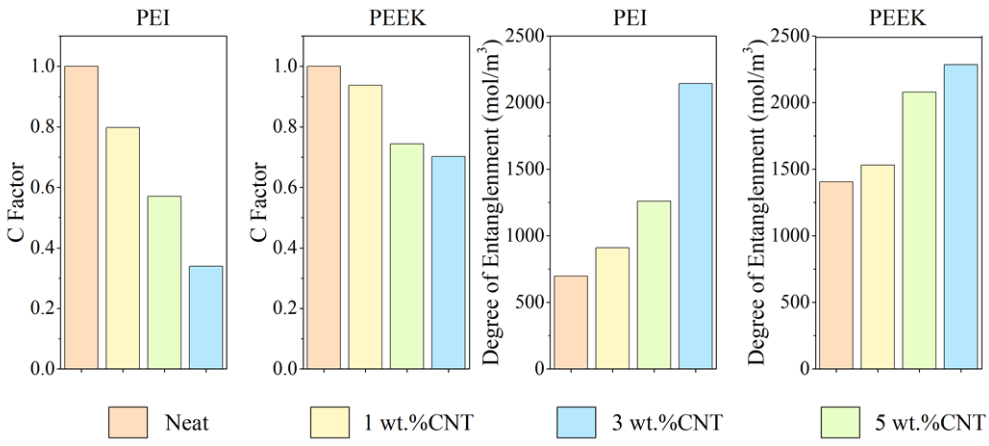

Figure 3.24 : C factor and degree of entanglement results of the samples.

The degree of entanglement was calculated by Eq. 3.5, of storage modulus in the rubbery region (R: gas constant, T: temperature in the rubbery region 230 °C for PEI 180 °C for PEEK) [33].

$$\text{Degree of entanglement}(N) = \frac{E'}{6RT}\,\text{mol}/m^3 \tag{3.5}$$

The results showed with an increase in CNT content, the degree of entanglement in CNT/PEI and CNT/PEEK composites were increased supporting the good CNT-polymer interaction as similar to CNT/PP and CNT-ABS composites (see Fig. 3.24) [21, 33].

Moreover, the adhesion factor was calculated for CNT reinforced PEI and PEEK composites. Calculations were performed by tan delta at T_g and volume fraction of the CNT according to the Eq. 3.6 below.

$$\text{Adhesion factor } (A) = \frac{1}{(1-\phi_f)}\frac{\tan\delta_c}{\tan\delta_p} - 1 \tag{3.6}$$

As the interaction between CNT and polymer increases, the adhesion factor is expected to decrease. For CNT/PEI and CNT/PEEK composites, the adhesion factor decreased with the increasing CNT content, and the lowest adhesion factors were obtained from 5 wt.% CNT reinforced PEI and PEEK composites as -0.37 and -0.14, respectively (see Fig. 3.25).

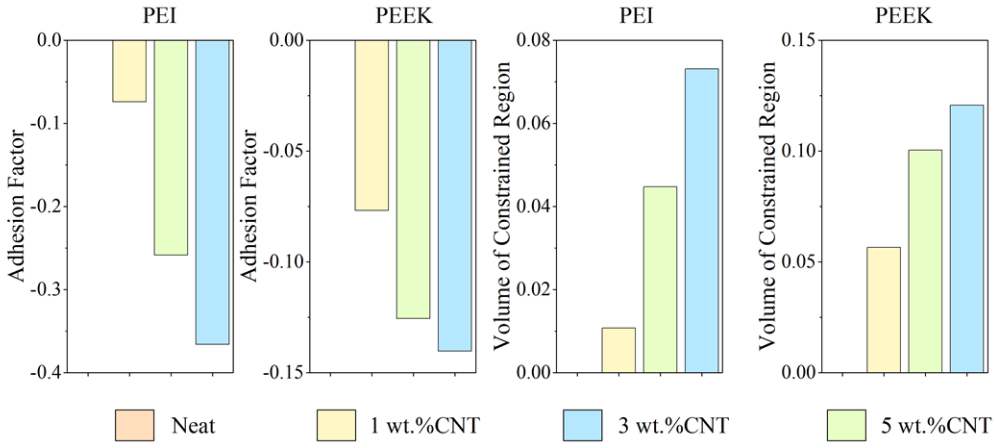

Figure 3.25 : Adhesion factor and volume of constrained region results of the samples.

Also, the lower mobility of chains when CNT were calculated by utilizing Eq. 3.7. As discussed before, the decrease in the height and under the area of the tan delta

curve with the CNT reinforcement were indications that the polymer mobility of the CNT was restricted, that is, the fillers constrained a certain region. Thus, for further calculations, tan delta at T_g was employed and energy loss fraction of neat polymer and composites represented as W_0 and W, respectively were found according to Eq.3.7. In the equations, C_v and C_0 (C_0 was taken as 0) were named as the volume of the constrained region of composites and the neat polymer, respectively. By rearranging Eq. 3.7 with Eq. 3.8, Eq. 3.9 was obtained and calculated accordingly.

$$\mathrm{W} = \frac{\pi \tan \delta}{\pi \tan \delta + 1} \tag{3.7}$$

$$\mathrm{W} = \frac{(1 - \mathrm{C_V})\,\mathrm{W_0}}{(1 - \mathrm{C_0})} \tag{3.8}$$

$$\mathrm{C_V} = 1 - \frac{(1 - \mathrm{C_0})\,\mathrm{W}}{\mathrm{W_0}} \tag{3.9}$$

An increase in the constrained region of the polymers with CNT reinforcement were clearly observed and the maximum constrained region values were calculated as 0.07 and 0.12 from 5 wt.% CNT/PEI and 5 wt.% CNT/PEEK composites, respectively (see Fig. 3.25).

3.6 Heat Deflection Temperature of CNT/PEI and CNT/PEEK Composites

HDT determination is one of the effective tools used to reveal the physical performance of polymers and polymer composites. Also, it is especially critical for high-performance thermoplastics produced by injection moldings such as PEI and PEEK, as the increase in HDT results in a faster injection process. In this section, The HDT of neat PEI and PEEK were measured as 204 °C and 190 °C, respectively, and the highest HDT was obtained from 5 wt.% CNT/PEI and 5 wt.% CNT/PEEK composites as 207 °C and 219 °C increasing by 3 °C and 29 °C, respectively ((see Table 3.8)). Higher increment in PEEK samples may be attributed to and increase in crystalline fraction with the presence of CNT and less void content. With the presence of CNT an increase in HDT was indicative of improved thermal properties and a good CNT-polymer interface which is important for processing and the performance (see Fig. 3.26) [104].

Table 3.8 : HDT of neat PEI, PEEK and their CNT reinforced composites.

CNT content (wt.%)	HDT of PEI (°C)	HDT of PEEK (°C)
0	204	190
1	205	210
3	204	218
5	207	219

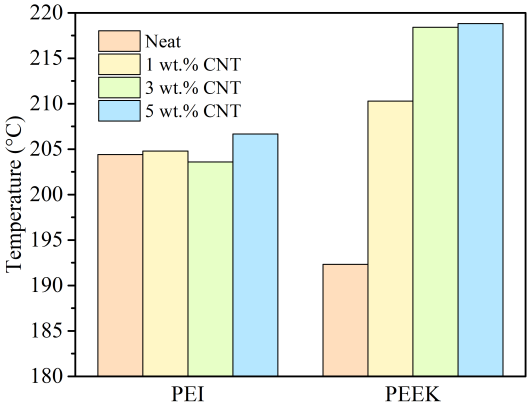

Figure 3.26 : HDT of CNT/PEI and CNT/PEEK composites.

3.7 Flexural Modulus of CNT/PEI and CNT/PEEK Composites

It is important to improve the mechanical properties of polymers to bring them multifunctional properties, thus, flexural testing of neat PEI, PEEK, and their CNT reinforced composites were performed to evaluate the effect of CNT on the overall mechanical properties of polymer composites. The flexural modulus of the neat PEI and PEEK were found to be 2.76 and 2.95 GPa, respectively (see Table. 3.9). When compared with earlier studies performed with injection molding, the neat PEI and PEEK modulus was lower in this study. Hence, the results may be affected due to the processing technique in which a driven pressure of the polymer through a die is not present. So the resulting composites presents more voids and irregularities [105–107]. On the other hand, revealing the CNT on flexural modulus, the modulus were both increased in CNT/PEI and CNT/PEEK composites. The highest modulus was obtained from 5 wt.% CNT/PEI and 5 wt.% CNT/PEEK composites as 3.38 and 3.77 GPa, with 22% and 28% increment, respectively (see Fig. 3.27). In addition, examining the effect of 1 and 3 wt.% CNT on the polymers, CNT provided a further increase in the

flexural modulus of PEEK, which is also related to the increase in the crystal fraction of CNT and its less void content. The improvement of the mechanical properties of the polymers by CNT reinforcement indicated that the interaction between CNT and polymers is high and a good interface is formed between the CNT and polymers [80, 108].

Table 3.9 : Flexural modulus of neat PEI, PEEK and their CNT reinforced composites.

CNT content (wt.%)	Flexural Modulus of PEI (GPa)	Flexural Modulus of PEEK (GPa)
0	2.76	2.95
1	2.73	3.27
3	2.83	3.72
5	3.38	3.77

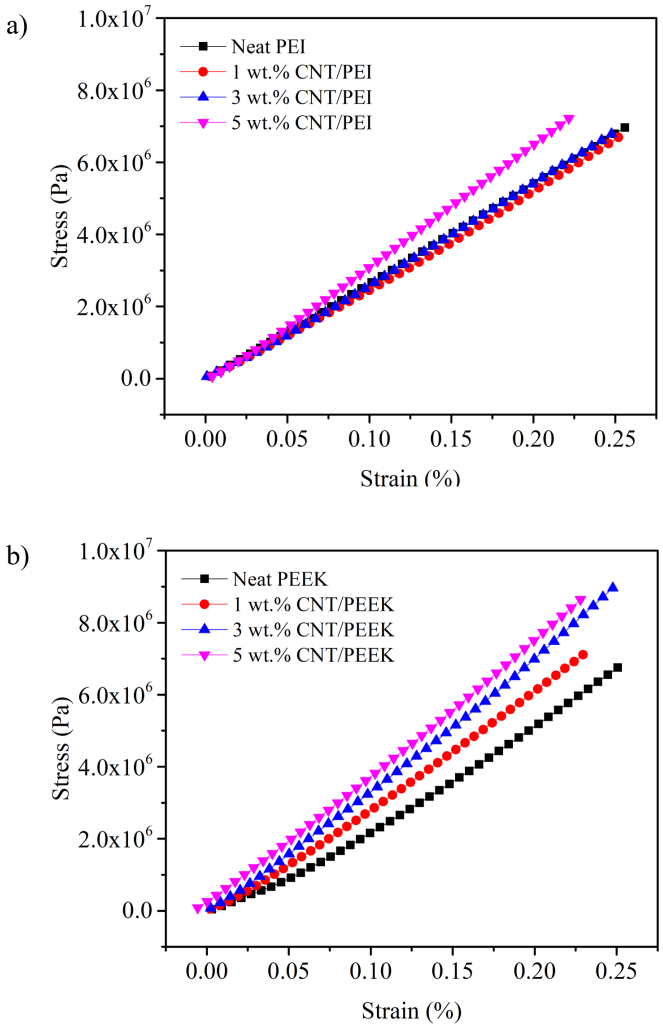

Figure 3.27 : Stress-strain curve for (a) CNT/PEI and (b) CNT/PEEK composites.

4. CONCLUSION

In this study, 1, 3, and 5 wt.% CNT reinforced PEI and PEEK composites were successfully produced with a twin-screw extruder. The thermal, morphological, viscoelastic, and mechanical properties of the produced composites were examined in detail. According to TGA and DSC results, no significant effect of CNT on T_g and decomposition temperature of PEI and PEEK was observed, however, CNT as acting nucleation side increased crystalline fraction of PEEK, and higher crystallinity was obtained from 1 wt.% CNT/PEEK composites as 29%. The morphological analysis revealed that CNT reinforced PEI and PEEK composites were fabricated homogeneously without any agglomerations. However, CNT reinforced PEI composites presented voids and less dispersion efficiency of CNT as in-line with the DMA results. Additionally, critical strain decreased and the Payne effect was more pronounced with CNT presence. Also, it increased the storage modulus and complex viscosity of PEI and PEEK depending on frequency. Frequency dependency of storage modulus disappeared and shear thinning behavior became more dominant with increasing CNT loading and the percolation threshold was found below 1 wt.% for both polymers. The thermo-mechanical properties of CNT/PEI and CNT/PEEK composites showed a coherency with the CNT concentration on the enhancement of storage modulus and decrease in tan delta of them. It is also shown that the increase in storage modulus of CNT/PEEK composites were higher than CNT/PEI ones, due to an increase in a crystalline fraction of PEI thanks to the presence of CNT. Analyzing the CNT polymer interaction mathematically using DMA data, the C factor and adhesion factor decreased with the amount of CNT, and the degree of entanglement and volume of the constrained region increased. The best results were obtained from 5 wt.% CNT/PEI and 5 wt.% CNT/PEEK composites having C factor of 0.27 and 0.30, and constrained regions of 0.07 and 0.12, respectively. It was also reported that CNT increased the HDT of PEI and PEEK by 3 and 29°C, respectively, at 5% CNT reinforcement. The reason for the increase in PEEK samples is related to the increase

in the crystal fraction of CNT. The CNT reinforcement increased HDT, which is an indicator that it improves the thermal properties. It is important for the analysis of the performance of the part to be used as a structural part under temperature and for the faster molding time of the materials to be produced by injection molding. Also, the flexural modulus which is important for materials that can be multifunctional were analyzed. The CNT increased the flexural modulus of the neat PEI and PEEK, which is the sign of well filler-polymer interphase, and the highest modulus was obtained from 5 wt.% CNT/PEI and 5 wt.% CNT/PEEK as 3.38 ve 3.77 GPa. As a result, viscoelastic properties of CNT reinforced PEI and PEEK composites were evaluated by oscillator rheology analysis and DMA, and it was revealed that CNT-polymer interaction increased with increasing CNT content.

REFERENCES

[1] **Rana, S.**, **Alagirusamy, R. and Joshi, M.** (2009). A review on carbon epoxy nanocomposites, *Journal of Reinforced Plastics and Composites*, *28*(4), 461–487.

[2] **Montazeri, A.**, **Pourshamsian, K. and Riazian, M.** (2012). Viscoelastic properties and determination of free volume fraction of multi-walled carbon nanotube/epoxy composite using dynamic mechanical thermal analysis, *Materials & Design (1980-2015)*, *36*, 408–414.

[3] **Montazeri, A. and Montazeri, N.** (2011). Viscoelastic and mechanical properties of multi walled carbon nanotube/epoxy composites with different nanotube content, *Materials & Design*, *32*(4), 2301–2307.

[4] **Fogel, M.**, **Parlevliet, P.**, **Geistbeck, M.**, **Olivier, P. and Dantras, E.** (2015). Thermal, rheological and electrical analysis of MWCNTs/epoxy matrices, *Composites Science and Technology*, *110*, 118–125.

[5] **Chandrasekaran, S.**, **Seidel, C. and Schulte, K.** (2013). Preparation and characterization of graphite nano-platelet (GNP)/epoxy nano-composite: Mechanical, electrical and thermal properties, *European Polymer Journal*, *49*(12), 3878–3888.

[6] **Tang, L.C.**, **Wan, Y.J.**, **Yan, D.**, **Pei, Y.B.**, **Zhao, L.**, **Li, Y.B.** ..... **Lai, G.Q.** (2013). The effect of graphene dispersion on the mechanical properties of graphene/epoxy composites, *Carbon*, *60*, 16–27, 03.050.

[7] **Cao, G.** (2016). Multi-functional epoxy/graphene nanoplatelet composites (*PhD Dissertation)*, The University of Manchester, Faculty of Engineering and Physical Sciences, United Kingdom.

[8] **Wang, F.**, **Drzal, L.T.**, **Qin, Y. and Huang, Z.** (2015). Mechanical properties and thermal conductivity of graphene nanoplatelet/epoxy composites, *Journal of materials science*, *50*(3), 1082–1093.

[9] **Liu, Y. and Wilkinson, A.** (2018). Rheological percolation behaviour and fracture properties of nanocomposites of MWCNTs and a highly crosslinked aerospace-grade epoxy resin system, *Composites Part A: Applied Science and Manufacturing*, *105*, 97–107.

[10] **Kim, J.A.**, **Seong, D.G.**, **Kang, T.J. and Youn, J.R.** (2006). Effects of surface modification on rheological and mechanical properties of CNT/epoxy composites, *Carbon*, *44*(10), 1898–1905.

[11] **Ma, P.C.**, **Mo, S.Y.**, **Tang, B.Z. and Kim, J.K.** (2010). Dispersion, interfacial interaction and re-agglomeration of functionalized carbon nanotubes in epoxy composites, *Carbon*, *48*(6), 1824–1834.

[12] **Sodeifian, G.**, **Nikooamal, H.R. and Yousefi, A.A.** (2012). Molecular dynamics study of epoxy/clay nanocomposites: rheology and molecular confinement, *Journal of Polymer Research*, *19*(6), 1–12.

[13] **Hiremath, V. and Shukla, D.K.** (2020). Rheological properties and curing behaviour of Epoxy-alumina nanocomposites, *Materials Today: Proceedings*, *22*, 2732–2740.

[14] **Yue, L.** (2018). Biobased Epoxy Composites: Sustainable Alternative for Advanced Materials, (*PhD Dissertation)*, Case Western Reserve University, Cleveland.

[15] **Zhu, J.**, **Wei, S.**, **Yadav, A. and Guo, Z.** (2010). Rheological behaviors and electrical conductivity of epoxy resin nanocomposites suspended with in-situ stabilized carbon nanofibers, *Polymer*, *51*(12), 2643–2651.

[16] **Seyhan, A.T.**, **Gojny, F.**, **Tanoğlu, M. and Schulte, K.** (2007). Rheological and dynamic-mechanical behavior of carbon nanotube/vinyl ester–polyester suspensions and their nanocomposites, *European Polymer Journal*, *43*(7), 2836–2847.

[17] **Urena-Benavides, E.E.**, **Kayatin, M.J. and Davis, V.A.** (2013). Dispersion and rheology of multiwalled carbon nanotubes in unsaturated polyester resin, *Macromolecules*, *46*(4), 1642–1650.

[18] **Ibeh, C.C.** (2011). *Thermoplastic materials: properties, manufacturing methods, and applications*, CRC Press.

[19] **Arrigo, R. and Malucelli, G.** (2020). Rheological behavior of polymer/carbon nanotube composites: an overview, *Materials*, *13*(12), 2771.

[20] **Biron, M.**, (2016). Thermoplastic Specific Properties, *Material Selection for Thermoplastic Parts,* William Andrew Publishing, 39–75.

[21] **Jyoti, J.**, **Singh, B.P.**, **Arya, A.K. and Dhakate, S.** (2016). Dynamic mechanical properties of multiwall carbon nanotube reinforced ABS composites and their correlation with entanglement density, adhesion, reinforcement and C factor, *RSC advances*, *6*(5), 3997–4006.

[22] **Gao, C.**, **Zhang, S.**, **Wang, F.**, **Wen, B.**, **Han, C.**, **Ding, Y. and Yang, M.** (2014). Graphene networks with low percolation threshold in ABS nanocomposites: selective localization and electrical and rheological properties, *ACS applied materials & interfaces*, *6*(15), 12252–12260.

[23] **Du, F.**, **Scogna, R.C.**, **Zhou, W.**, **Brand, S.**, **Fischer, J.E. and Winey, K.I.** (2004). Nanotube networks in polymer nanocomposites: rheology and electrical conductivity, *Macromolecules*, *37*(24), 9048–9055.

[24] **Sathyanarayana, S.**, **Olowojoba, G.**, **Weiss, P.**, **Pataki, B.**, **Mikonsaari, I.**, **Hübner, C. and Henning, F.** (2013). Twin-Screw compounding extrusion of Polystyrene (PS)/Multi walled carbon nanotube (MWCNT) nanocomposites with varying process: Comprehensive integration of morphology, interfacial behavior, thermal stability, rheology and electrical resistivity, *MACROMOLECULAR MATERIALS AND ENGINEERING*, *298*(1), 89–105.

[25] **Kota, A.K.**, **Cipriano, B.H.**, **Duesterberg, M.K.**, **Gershon, A.L.**, **Powell, D.**, **Raghavan, S.R. and Bruck, H.A.** (2007). Electrical and rheological percolation in polystyrene/MWCNT nanocomposites, *Macromolecules*, *40*(20), 7400–7406.

[26] **McClory, C.**, **Pötschke, P. and McNally, T.** (2011). Influence of Screw Speed on Electrical and Rheological Percolation of Melt-Mixed High-Impact Polystyrene/MWCNT Nanocomposites, *Macromolecular Materials and Engineering*, *296*(1), 59–69.

[27] **Pötschke, P.**, **Fornes, T. and Paul, D.** (2002). Rheological behavior of multiwalled carbon nanotube/polycarbonate composites, *Polymer*, *43*(11), 3247–3255.

[28] **Sung, Y.**, **Kum, C.**, **Lee, H.**, **Byon, N.**, **Yoon, H.G. and Kim, W.N.** (2005). Dynamic mechanical and morphological properties of polycarbonate/multi-walled carbon nanotube composites, *Polymer*, *46*(15), 5656–5661.

[29] **Gao, X.**, **Isayev, A.I. and Yi, C.** (2016). Ultrasonic treatment of polycarbonate/carbon nanotubes composites, *Polymer*, *84*, 209–222.

[30] **Isayev, A.**, **Kumar, R. and Lewis, T.M.** (2009). Ultrasound assisted twin screw extrusion of polymer–nanocomposites containing carbon nanotubes, *Polymer*, *50*(1), 250–260.

[31] **Kaynan, O.**, **Yıldız, A.**, **Bozkurt, Y.E.**, **Yenigun, E.O. and Cebeci, H.** (2020). Electrically conductive high-performance thermoplastic filaments for fused filament fabrication, *Composite Structures*, *237*, 111930.

[32] **Dean, K.**, **Yu, L. and Wu, D.Y.** (2007). Preparation and characterization of melt-extruded thermoplastic starch/clay nanocomposites, *Composites Science and Technology*, *67*(3-4), 413–421.

[33] **Verma, P.**, **Verma, M.**, **Gupta, A.**, **Chauhan, S.S.**, **Malik, R.S. and Choudhary, V.** (2016). Multi walled carbon nanotubes induced viscoelastic response of polypropylene copolymer nanocomposites: Effect of filler loading on rheological percolation, *Polymer Testing*, *55*, 1–9.

[34] **Kang, D.**, **Hwang, S.**, **Jung, B. and Shim, J.** (2021). Characterizations of polypropylene/single-walled carbon nanotube nanocomposites prepared by the novel melt processing technique with a controlled residence time, *Processes*, *9*(8), 1395.

[35] **Bai, J.**, **Goodridge, R.D.**, **Hague, R.J.**, **Song, M. and Okamoto, M.** (2014). Influence of carbon nanotubes on the rheology and dynamic mechanical properties of polyamide-12 for laser sintering, *Polymer Testing*, *36*, 95–100.

[36] **Wang, M.**, **Wang, W.**, **Liu, T. and Zhang, W.D.** (2008). Melt rheological properties of nylon 6/multi-walled carbon nanotube composites, *Composites Science and Technology*, *68*(12), 2498–2502.

[37] **Lee, K.P.M.**, **Brandt, M.**, **Shanks, R. and Daver, F.** (2020). Rheology and 3D Printability of Percolated Graphene–Polyamide-6 Composites, *Polymers*, *12*(9), 2014.

[38] **Han, M.S.**, **Lee, Y.K.**, **Lee, H.S.**, **Yun, C.H. and Kim, W.N.** (2009). Electrical, morphological and rheological properties of carbon nanotube composites with polyethylene and poly (phenylene sulfide) by melt mixing, *Chemical engineering science*, *64*(22), 4649–4656.

[39] **Diez-Pascual, A.M.**, **Naffakh, M.**, **Marco, C. and Ellis, G.** (2012). Rheological and tribological properties of carbon nanotube/thermoplastic nanocomposites incorporating inorganic fullerene-like WS2 nanoparticles, *The Journal of Physical Chemistry B*, *116*(27), 7959–7969.

[40] **Díez-Pascual, A.M.**, **Naffakh, M.**, **Gómez, M.A.**, **Marco, C.**, **Ellis, G.**, **Martínez, M.T.** ..... **Simard, B.** (2009). Development and characterization of PEEK/carbon nanotube composites, *Carbon*, *47*(13), 3079–3090, 07.020.

[41] **Alvaredo, Á.**, **Martín, M.I.**, **Castell, P.**, **Guzmán de Villoria, R. and Fernández-Blázquez, J.P.** (2019). Non-isothermal crystallization behavior of PEEK/graphene nanoplatelets composites from melt and glass states, *Polymers*, *11*(1), 124.

[42] **Yaragalla, S.**, **Zahid, M.**, **Panda, J.K.**, **Tsagarakis, N.**, **Cingolani, R. and Athanassiou, A.** (2021). Comprehensive Enhancement in Thermomechanical Performance of Melt-Extruded PEEK Filaments by Graphene Incorporation, *Polymers*, *13*(9), 1425.

[43] **Bangarusampath, D.**, **Ruckdäschel, H.**, **Altstädt, V.**, **Sandler, J.K.**, **Garray, D. and Shaffer, M.S.** (2009). Rheology and properties of melt-processed poly (ether ether ketone)/multi-wall carbon nanotube composites, *Polymer*, *50*(24), 5803–5811.

[44] **Yuan, X.**, **Zhang, X.**, **Sun, L.**, **Wei, Y. and Wei, X.** (2019). Cellular toxicity and immunological effects of carbon-based nanomaterials, *Particle and fibre toxicology*, *16*(1), 1–27.

[45] **Somorjai, G.A. and Chaudret, B.** (2012). *Nanomaterials in Catalysis*, John Wiley & Sons.

[46] **Bigg, D.** (1984). An investigation of the effect of carbon black structure, polymer morphology, and processing history on the electrical conductivity

of carbon-black-filled thermoplastics, *Journal of Rheology*, *28*(5), 501–516.

[47] **Balasooriya, W.**, **Schrittesser, B.**, **Pinter, G.**, **Schwarz, T. and Conzatti, L.** (2019). The effect of the surface area of carbon black grades on HNBR in harsh environments, *Polymers*, *11*(1), 61.

[48] **Pan, Y.**, **Schubert, D.W.**, **Ryu, J.E.**, **Wujick, E.**, **Liu, C.**, **Shen, C. and Liu, X.** (2018). Dynamic oscillatory rheological properties of polystyrene/poly (methyl methacrylate) blends and their composites in the presence of carbon black, *Engineered Science*, *1*(10), 86–94.

[49] **Zhang, Q.**, **Xiong, H.**, **Yan, W.**, **Chen, D. and Zhu, M.** (2008). Electrical conductivity and rheological behavior of multiphase polymer composites containing conducting carbon black, *Polymer Engineering & Science*, *48*(11), 2090–2097.

[50] **Kim, Y.A.**, **Hayashi, T.**, **Endo, M. and Dresselhaus, M.S.**, (2013). Carbon nanofibers, Springer handbook of nanomaterials, Springer, pp.233–262.

[51] **Marcaníková, L.**, **Hausnerová, B. and Kitano, T.** (2009). Rheological Behavior of Composites Based on Carbon Fibers Recycled from Aircraft Waste, *AIP Conference Proceedings*, volume1152, American Institute of Physics, pp.234–247.

[52] **Naseri, A.**, **Samadi, M.**, **Ebrahimi, M.**, **Kheirabadi, M. and Moshfegh, A.Z.**, (2020). Heterogeneous photocatalysis by organic materials: from fundamental to applications, Current Developments in Photocatalysis and Photocatalytic Materials, Elsevier, pp.457–473.

[53] **Scaria, J.**, **Karim, A.V.**, **Divyapriya, G.**, **Nidheesh, P. and Kumar, M.S.**, (2020). Carbon-supported semiconductor nanoparticles as effective photocatalysts for water and wastewater treatment, Nano-Materials as Photocatalysts for Degradation of Environmental Pollutants, Elsevier, pp.245–278.

[54] **Miranda, A.N.d.**, **Pardini, L.C.**, **Santos, C.A.M.d. and Vieira, R.** (2011). Evaluation of carbon fiber composites modified by in situ incorporation of carbon nanofibers, *Materials Research*, *14*, 560–563.

[55] **Ceccia, S.**, **Ferri, D.**, **Tabuani, D. and Maffettone, P.L.** (2008). Rheology of carbon nanofiber-reinforced polypropylene, *Rheologica acta*, *47*(4), 425–433.

[56] **Bai, Q.q.**, **Wei, X.**, **Yang, J.h.**, **Zhang, N.**, **Huang, T.**, **Wang, Y. and Zhou, Z.w.** (2017). Dispersion and network formation of graphene platelets in polystyrene composites and the resultant conductive properties, *Composites Part A: Applied Science and Manufacturing*, *96*, 89–98.

[57] **Mousa, M.S.** (2018). Comparison between single-walled CNT, multi-walled CNT, and carbon nanotube-fiber pyrograf III, *IOP Conference Series: Materials Science and Engineering*, volume305, IOP Publishing, p.012025.

[58] **Kasgoz, A.**, **Akın, D. and Durmus, A.** (2014). Rheological and electrical properties of carbon black and carbon fiber filled cyclic olefin copolymer composites, *Composites Part B: Engineering*, *62*, 113–120.

[59] **Kasgoz, A.**, **Akın, D.**, **Ayten, A.I. and Durmus, A.** (2014). Effect of different types of carbon fillers on mechanical and rheological properties of cyclic olefin copolymer (COC) composites, *Composites Part B: Engineering*, *66*, 126–135.

[60] **Zhong, J.**, **Isayev, A.I. and Zhang, X.** (2016). Ultrasonic twin screw compounding of polypropylene with carbon nanotubes, graphene nanoplates and carbon black, *European Polymer Journal*, *80*, 16–39.

[61] **Pötschke, P.**, **Abdel-Goad*, M.**, **Pegel, S.**, **Jehnichen, D.**, **Mark, J.E.**, **Zhou**, D. and Heinrich, G.** (2009). Comparisons among electrical and rheological properties of melt-mixed composites containing various carbon nanostructures, *Journal of Macromolecular Science, Part A*, *47*(1), 12–19.

[62] **Lin, X.**, **Zhang, K.**, **Li, K. and Ren, D.** (2018). Dependence of rheological behaviors of polymeric composites on the morphological structure of carbonaceous nanoparticles, *Journal of Applied Polymer Science*, *135*(26), 46416.

[63] **Sumfleth, J.**, **Buschhorn, S.T. and Schulte, K.** (2011). Comparison of rheological and electrical percolation phenomena in carbon black and carbon nanotube filled epoxy polymers, *Journal of Materials Science*, *46*(3), 659–669.

[64] **Deng, H.**, **Skipa, T.**, **Zhang, R.**, **Lellinger, D.**, **Bilotti, E.**, **Alig, I. and Peijs, T.** (2009). Effect of melting and crystallization on the conductive network in conductive polymer composites, *Polymer*, *50*(15), 3747–3754.

[65] **Pötschke, P.**, **Abdel-Goad, M.**, **Alig, I.**, **Dudkin, S. and Lellinger, D.** (2004). Rheological and dielectrical characterization of melt mixed polycarbonate-multiwalled carbon nanotube composites, *Polymer*, *45*(26), 8863–8870.

[66] **Palacios, J.K.**, **Ben Fekih, A.**, **Yus Argon, C.**, **Irusta, S.**, **Jestin, S. and Dagréou, S.** (2021). Tailoring the rheology and electrical properties of polyamide 66 nanocomposites with hybrid filler approach: graphene and carbon nanotubes, *Polymer International*.

[67] **Beuguel, Q.**, **Mija, A.**, **Vergnes, B. and Peuvrel-Disdier, E.** (2018). Structural, thermal, rheological and mechanical properties of polypropylene/graphene nanoplatelets composites: Effect of particle size and melt mixing conditions, *Polymer Engineering & Science*, *58*(11), 1937–1944.

[68] **Rueda, M.M.**, **Auscher, M.C.**, **Fulchiron, R.**, **Perie, T.**, **Martin, G.**, **Sonntag, P. and Cassagnau, P.** (2017). Rheology and applications of highly filled polymers: A review of current understanding, *Progress in Polymer Science*, *66*, 22–53.

[69] **Knauert, S.T.**, **Douglas, J.F. and Starr, F.W.** (2007). The effect of nanoparticle shape on polymer-nanocomposite rheology and tensile strength, *Journal of Polymer Science Part B: Polymer Physics*, *45*(14), 1882–1897.

[70] **Amancio-Filho, S.T.**, **Roeder, J.**, **Nunes, S.P.**, **dos Santos, J.F. and Beckmann, F.** (2008). Thermal degradation of polyetherimide joined by friction riveting (FricRiveting). Part I: Influence of rotation speed", *Polym. Degrad. Stab.*, *93*(8), 1529–1538.

[71] **Vasconcelos, G.d.C.**, **Mazur, R.L.**, **Ribeiro, B.**, **Botelho, E.C. and Costa, M.L.** (2014). Evaluation of decomposition kinetics of poly (ether-ether-ketone) by thermogravimetric analysis, *Materials Research*, *17*, 227–235.

[72] **Patel, P.**, **Hull, T.R.**, **McCabe, R.W.**, **Flath, D.**, **Grasmeder, J. and Percy, M.** (2010). Mechanism of thermal decomposition of poly(ether ether ketone) (PEEK) from a review of decomposition studies, *Polymer Degradation and Stability*, *95*(5), 709–718.

[73] **Huang, C.**, **Qian, X. and Yang, R.** (2018). Thermal conductivity of polymers and polymer nanocomposites, *Materials Science and Engineering: R: Reports*, *132*, 1–22.

[74] **Georgiev, V.** (2021). Preparation and thermal stability evaluation of GNP/CNT doped poly (lactic acid) and high-density polyethylene nanocomposites, *BULGARIAN CHEMICAL COMMUNICATIONS*, 249.

[75] **Rinaldi, M.**, **Ghidini, T. and Nanni, F.** (2021). Fused filament fabrication of polyetheretherketone/multiwalled carbon nanotube nanocomposites: the effect of thermally conductive nanometric filler on the printability and related properties, *Polymer International*.

[76] **Ribeiro, B.**, **Santos, L.**, **Santos, A.**, **Costa, M. and Botelho, E.** (2019). Thermal decomposition kinetic study of multiwalled carbon nanotube buckypaper-reinforced poly (ether-imide) composites, *Journal of Thermoplastic Composite Materials*, *32*(1), 62–75.

[77] **Klonos, P.A.**, **Tegopoulos, S.N.**, **Koutsiara, C.S.**, **Kontou, E.**, **Pissis, P. and Kyritsis, A.** (2019). Effects of CNTs on thermal transitions, thermal diffusivity and electrical conductivity in nanocomposites: comparison between an amorphous and a semicrystalline polymer matrix, *Soft Matter*, *15*(8), 1813–1824.

[78] **Ma, Q.**, **Georgiev, G. and Cebe, P.** (2011). Constraints in semicrystalline polymers: Using quasi-isothermal analysis to investigate the mechanisms of formation and loss of the rigid amorphous fraction, *Polymer*, *52*(20), 4562–4570.

[79] **Shang, Y.**, **Wu, X.**, **Liu, Y.**, **Jiang, Z.**, **Wang, Z.**, **Jiang, Z. and Zhang, H.** (2019). Preparation of PEEK/MWCNTs composites with excellent mechanical and tribological properties, *High Performance Polymers*, *31*(1), 43–50.

[80] **Pitchan, M.K.**, **Bhowmik, S.**, **Balachandran, M. and Abraham, M.** (2016). Effect of surface functionalization on mechanical properties and decomposition kinetics of high performance polyetherimide/MWCNT nano composites, *Composites Part A: Applied Science and Manufacturing*, *90*, 147–160.

[81] **Awaja, F. and Zhang, S.** (2015). Self-bonding of PEEK for active medical implants applications, *Journal of Adhesion Science and Technology*, *29*(15), 1593–1606.

[82] **Soudmand, B.H.**, **Shelesh-Nezhad, K. and Salimi, Y.** (2020). A combined differential scanning calorimetry-dynamic mechanical thermal analysis approach for the estimation of constrained phases in thermoplastic polymer nanocomposites, *Journal of Applied Polymer Science*, *137*(41), 49260.

[83] **Rong, C.**, **Ma, G.**, **Zhang, S.**, **Song, L.**, **Chen, Z.**, **Wang, G. and Ajayan, P.** (2010). Effect of carbon nanotubes on the mechanical properties and crystallization behavior of poly (ether ether ketone), *Composites Science and Technology*, *70*(2), 380–386.

[84] **Durmus, A.**, **Kasgoz, A. and Macosko, C.W.** (2007). Linear low density polyethylene (LLDPE)/clay nanocomposites. Part I: Structural characterization and quantifying clay dispersion by melt rheology, *Polymer*, *48*(15), 4492–4502.

[85] **Payne, A. and Whittaker, R.** (1971). Low strain dynamic properties of filled rubbers, *Rubber chemistry and technology*, *44*(2), 440–478.

[86] **Kim, H. and Macosko, C.W.** (2009). Processing-property relationships of polycarbonate/graphene composites, *Polymer*, *50*(15), 3797–3809.

[87] **Ajinjeru, C.**, **Kishore, V.**, **Liu, P.**, **Lindahl, J.**, **Hassen, A.A.**, **Kunc, V.** ..... **Duty, C.** (2018). Determination of melt processing conditions for high performance amorphous thermoplastics for large format additive manufacturing, *Additive Manufacturing*, *21*, 125–132, 03.004.

[88] **Ajinjeru, C.**, **Kishore, V.**, **Lindahl, J.**, **Sudbury, Z.**, **Hassen, A.A.**, **Post,** B. ..... **Duty, C.** (2018). The influence of dynamic rheological properties on carbon fiber-reinforced polyetherimide for large-scale extrusion-based additive manufacturing, *The International Journal of Advanced Manufacturing Technology*, *99*(1), 411–418, 10.1007.

[89] **Kishore, V.**, **Ajinjeru, C.**, **Duty, C.E.**, **Hassen, A.A.**, **Lindahl, J.M.**, **Liu, P. and Kunc, V.** (2017). Rheological characteristics of fiber reinforced poly (ether ketone ketone)(PEKK) for melt extrusion additive manufacturing, **Technical Report**, Oak Ridge National Lab.(ORNL), Oak Ridge, TN (United States).

[90] **Ajinjeru, C.**, **Kishore, V.**, **Chen, X.**, **Hershey, C.**, **Lindahl, J.**, **Kunc, V.** ..... **Duty, C.** (2019). Rheological survey of carbon fiber-reinforced high-temperature thermoplastics for big area additive manufacturing

tooling applications, *Journal of Thermoplastic Composite Materials*, 0892705719873941.

[91] **Wan, T.**, **Clifford, M.**, **Gao, F.**, **Bailey, A.**, **Gregory, D. and Somsunan, R.** (2005). Strain amplitude response and the microstructure of PA/clay nanocomposites, *Polymer*, *46*(17), 6429–6436.

[92] **Nishitani, Y.**, **Yamanaka, T.**, **Kajiyama, T. and Kitano, T.** (2016). Rheological Properties of Carbon Nanofiber Filled Polyamide Composites and Blend of These Composites and TPE, *Viscoelastic and Viscoplastic Materials*, 103–140.

[93] **Cassagnau, P.** (2008). Melt rheology of organoclay and fumed silica nanocomposites, *Polymer*, *49*(9), 2183–2196.

[94] **Moniruzzaman, M. and Winey, K.I.** (2006). Polymer nanocomposites containing carbon nanotubes, *Macromolecules*, *39*(16), 5194–5205.

[95] **Arrigo, R.**, **Morici, E.**, **Cammarata, M. and Dintcheva, N.T.** (2017). Rheological percolation threshold in high-viscosity polymer/CNTs nanocomposites, *Journal of Engineering Mechanics*, *143*(5), D4016006.

[96] **Xu, X.**, **Chen, J. and An, L.** (2014). Shear thinning behavior of linear polymer melts under shear flow via nonequilibrium molecular dynamics, *The Journal of chemical physics*, *140*(17), 174902.

[97] **Li, S.P.**, **Zhao, G. and Chen, H.Y.** (2005). The relationship between steady shear viscosity and complex viscosity, *Journal of dispersion science and technology*, *26*(4), 415–419.

[98] **Prashantha, K.**, **Soulestin, J.**, **Lacrampe, M.F.**, **Claes, M.**, **Dupin, G. and Krawczak, P.** (2008). Multi-walled carbon nanotube filled polypropylene nanocomposites based on masterbatch route: Improvement of dispersion and mechanical properties through PP-g-MA addition, *Express Polymer Letters*, *2*(10), 735–745.

[99] **Han, C.D. and Jhon, M.S.** (1986). Correlations of the first normal stress difference with shear stress and of the storage modulus with loss modulus for homopolymers, *Journal of Applied Polymer Science*, *32*(3), 3809–3840.

[100] **Babal, A.S.**, **Singh, B.P.**, **Jyoti, J.**, **Sharma, S.**, **Arya, A.K. and Dhakate, S.R.** (2016). Synergistic effect on static and dynamic mechanical properties of carbon fiber-multiwalled carbon nanotube hybrid polycarbonate composites, *RSC advances*, *6*(72), 67954–67967.

[101] **Bergström, J.**, (2015). Experimental Characterization Techniques, *Mechanics of solid polymers: theory and computational modeling,* William Andrew, 19–114.

[102] **Ornaghi Jr, H.L.**, **Bolner, A.S.**, **Fiorio, R.**, **Zattera, A.J. and Amico, S.C.** (2010). Mechanical and dynamic mechanical analysis of hybrid

composites molded by resin transfer molding, *Journal of Applied Polymer Science*, *118*(2), 887–896.

[103] **Poletto, M. and Zattera, A.J.** (2017). Mechanical and dynamic mechanical properties of polystyrene composites reinforced with cellulose fibers: coupling agent effect, *Journal of Thermoplastic Composite Materials*, *30*(9), 1242–1254.

[104] **Sherif, G.**, **Chukov, D.I.**, **Tcherdyntsev, V.V.**, **Torokhov, V.G. and Zherebtsov, D.D.** (2020). Effect of glass fibers thermal treatment on the mechanical and thermal behavior of polysulfone based composites, *Polymers*, *12*(4), 902.

[105] **Sun, Z.**, **Zhao, Z.K.**, **Zhang, Y.Y.**, **Li, Y.Q.**, **Fu, Y.Q.**, **Sun, B.G.** ..... **Fu, S.Y.** (2021). Mechanical, tribological and thermal properties of injection molded short carbon fiber/expanded graphite/polyetherimide composites, *Composites Science and Technology*, *201*, 108498.

[106] **Puértolas, J.**, **Castro, M.**, **Morris, J.**, **Ríos, R. and Ansón-Casaos, A.** (2019). Tribological and mechanical properties of graphene nanoplatelet/PEEK composites, *Carbon*, *141*, 107–122.

[107] **Bledzki, A.K. and Faruk, O.** (2004). Wood fiber reinforced polypropylene composites: Compression and injection molding process, *Polymer-Plastics Technology and Engineering*, *43*(3), 871–888.

[108] **Arash, B.**, **Wang, Q. and Varadan, V.** (2014). Mechanical properties of carbon nanotube/polymer composites, *Scientific reports*, *4*(1), 1–8.

CURRICULUM VITAE

Name Surname : Fulden Kaygınok

Place and Date of Birth :

E-Mail :

EDUCATION :

- **B.Sc.** : 2019, Istanbul Technical University, Faculty of Chemical and Metallurgical, Department of Metallurgical and Materials Engineering
- **B.Sc.** : 2021, Istanbul Technical University, Faculty of Aeronautics and Astronautics, Department of Aeronautical Engineering

PROFESSIONAL EXPERIENCE AND REWARDS:

- 2019-2022 Researcher at ITU Aerospace Research Center
- 2020-2021 Boeing Student Scholarship
- 2019-2020 Researcher at BOEING-ITUARC project
- 2019 Award for being ranked 3rd among the fourth year undergraduate students in bachelor degree in Met. & Mat. Eng.

PUBLICATIONS, PRESENTATIONS AND PATENTS ON THE THESIS:

- **Kayginok F.**, Karabal M., Yildiz A., Yildiz K., Cebeci H., 2022. Establishing the polymer effect on the viscoelastic properties of CNTs reinforced PEI and PEEK, *ICCS25 - 25th International Conference on Composite Structures*, 19-22 July, 2022 Porto, Portugal (Oral Presentation)

OTHER PUBLICATIONS, PRESENTATIONS AND PATENTS:

- Bozkurt Y.E, Kaynan O., Yildiz A., Ozden Y. E., Cebeci F. C., Cebeci H., Akar E., **Kaygınok F**., Kızılcık G., Solak N., 2019. BN/HDPE and BN/PEI Composites for Thermal Management Applications. *International Conference of The Polymer Processing Society*, 26-30 May, 2019 Izmir, Turkey. (Oral Presentation)